A discrete particle model reproducing collective dynamics of a bee swarm

A discrete particle model reproducing collective dynamics of a bee swarm

Sara Bernardi[1], Annachiara Colombi[2] and Marco Scianna[3]

Department of Mathematical Sciences, Politecnico di Torino, Corso Duca degli Abruzzi 24, 10129 Torino, Italy

Abstract

In this article, we present a microscopic discrete mathematical model describing collective dynamics of a bee swarm. More specifically, each bee is set to move according to individual strategies and social interactions, the former involving the desire to reach a target destination, the latter accounting for repulsive/attractive stimuli and for alignment processes. The insects tend in fact to remain sufficiently close to the rest of the population, while avoiding collisions, and they are able to track and synchronize their movement to the flight of a given set of neighbors within their visual field. The resulting collective behavior of the bee cloud therefore emerges from non-local short/long-range interactions. Differently from similar approaches present in the literature, we here test different alignment mechanisms (i.e., based either on an Euclidean or on a topological neighborhood metric), which have an impact also on the other social components characterizing insect behavior. A series of numerical realizations then shows the phenomenology of the swarm (in terms of pattern configuration, collective productive movement, and flight synchronization) in different regions of the space of free model parameters (i.e., strength of attractive/repulsive forces, extension of the interaction regions). In this respect, constraints in the possible variations of such coefficients are here given both by reasonable empirical observations and by analytical results on some stability characteristics of the defined pairwise interaction kernels, which have to assure a realistic crystalline configuration of the swarm. An analysis of the effect of unconscious random fluctuations

[1]E-Mail: s.bernardi@unito.it
[2]E-Mail: annachiara.colombi@polito.it
[3]E-Mail: marco.scianna@polito.it

of bee dynamics is also provided.

Keywords: Bee swarm, Collective dynamics, Swarming, H-stability, Alignment mechanisms

---

1. Introduction

Self-organization and collective dynamics and behavior are ubiquitous phenomena in many biological and physical systems formed by populations of individuals, e.g., from colonies of bacteria to human crowds, see, for instance, [9], [32], [44] and references therein. The description of swinging and coordinate movements of groups of animals, such as birds, fishes, insects, or certain mammals, has indeed increased in the last decades the multidisciplinary interest of various research communities, e.g., biologists, ecologists, sociologists, and applied mathematicians.

In this perspective, the theoretical and computational literature presents a wide range of approaches. For instance, in *discrete models*, characteristic of a *microscopic* point of view, the interacting individuals are described by localized particles, which move according to individual rules involving their position and velocity (or acceleration). The evolution of the overall system is indeed defined by proper sets of (first or second order) ordinary differential equations (ODEs). In this respect, discrete approaches are able to provide a detailed description of the dynamics of each agent and therefore represent a natural tool to investigate animal world-related collective phenomena (see, for instance, [10], [16], [17], [23], [26], [28], [31], [36], [38]).

However, when the number of component particles is significantly large, as in the case of fishes [37] or myxobacteria [29], [33], the solution of the resulting system of ODEs becomes computationally expensive and therefore different methods are needed. In this respect, *continuous models*, characteristic of a *macroscopic* point of view, rely on the definition of a proper density of agents, which evolves following (typically nonlinear) partial differential equations (PDEs). They are indeed based on conservation laws and phenomenological assumptions for their closure, see for example [3], [45], [46], [47]. It is useful to remark that the rules of motion underlying discrete and continuous approaches often coincide: however, in the former case, they are related to the behavior of the single agents, whereas, in the second case, they account for the dynamics of the overall population density.

A bridge between the microscopic word and the macroscopic representation of the system is represented by *kinetic* models. Characteristics of a *mesoscopic* point of view, they are able to derive, employing hydrodynamic arguments, Boltzmann-like evolution laws for statistical distribution functions which describe the position and velocity of the components of the population of interest [5], [7], [34].

Some of the previous-cited mathematical approaches deal with the collective behavior of bee swarms, which represent an interesting problem to be studied. Such insect populations, which are typically composed by the old queen and by 10000 to 30000 worker individuals, in fact undergo a synchronized flight when they have the specific purpose of reaching the new nest site [42]. All colonies are subjected to this natural phenomenon, and every year beekeepers have to deal with it in late spring and early summer. In this period, as the weather warms up and flowers begin to bloom, the colony is in fact at the peak of its capacity and ready to produce a new hive. Entering in more details, when the migrating bees leave the original hive they first temporarily settle on a tree branch a few meters away from the old nest. There, they cluster around the queen, and a given set of bees (called *scout*) starts exploring the surrounding area. Each of the scout individuals finds a suitable location for the community to live: then, it returns to the rest of the population and performs the waggle dance to broadcast the information about the possible new nest, e.g., how suitable it is for the colony. Nest proposals coming from the scout bees may be different but, after some hours (sometimes days), an agreement is finally found. The whole swarm, organized in a well-defined pattern, finally takes off and flies towards the chosen destination, following the guidance of the scout/informed individuals (see [42] for more details).

Selected characteristics of such a bee collective migration are here reproduced by a microscopic-discrete approach. In particular, the component insects of a representative swarm are individually described by their position and velocity. Each bee is then set to behave following an individual strategy, i.e., the aim to reach a target destination, and social interactions. The latter involves repulsive/attractive stimuli (the desire to remain close to the rest of the population while maintaining a comfort space), as well as the ability of bees to synchronize their movement with a given set of surrounding individuals. Such insect behavioral rules have been of course previously proposed in the computational literature (cf. [17], [18], [26], [28], see the conclusive section for more detailed comments): however, we here test and provide a

comparison, in terms of numerical outcomes relative to selected swarming characteristics, of different combinations of alternative assumptions underlying flight alignment mechanisms and bee pairwise interactions. Further, theoretical results are used to derive proper parameter estimate.

Entering in more details, the rest of this paper is organized as follows. In Section 2, we clarify the assumptions on which our mathematical approach is based and present the model components. More specifically, we first explain the characteristic representation of model bees; then, we give the equations of motion and introduce the relative velocity components. Sections 3 deals with different assumptions underlying flight synchronization mechanisms. In particular, we focus either on an Euclidean metric-based or on a topological neighborhood metric-based alignment process within the swarm. In this respect, we discuss how these two mutually exclusive hypothesis impact on the repulsion/attraction velocity contributions (which in turn have to satisfy a stability condition to assure a realistic crystalline patterning of the particle system). Different series of numerical realizations then analyze the swarm behavior in different parameter regimes and show that our approach is able to capture selected experimentally-observed swarm phenomenology (e.g., flight synchronization and productive motion). After discussing in Section 4 the effect of the inclusion of random contributions on the particle system, we review in Section 5 the results obtained in this paper. Finally, we compare our approach with similar discrete models presented in the literature dealing with bee dynamics and propose some possible improvements and developments of the work.

2. Mathematical model

2.1. Bee representation and characteristics

A population of N bees is modeled in the two-dimensional space $\mathbb{R}^2$. We are indeed considering a planar section, parallel to the ground, of a typical swarm (see Fig. 1, left panel). Each bee $i = 1, ..., N$ is intended as an autonomous particle and represented by a dimensionless material point with concentrated unitary mass. The generic i-th individual has the phase-space coordinates identified by $(\mathbf{x}_i(t), \mathbf{v}_i(t)) \in \mathbb{R}^{2\times 2}$, where the vectors $\mathbf{x}_i$, and $\mathbf{v}_i$ denote its actual position and velocity, respectively. We further define, for each insect i, a proper visual, as reproduced in Fig. 1, right panel:

$$\Omega_i^{\text{vis}}(t) = \left\{\mathbf{x} \in \mathbb{R}^2 : |\mathbf{x} - \mathbf{x}_i(t)| \leq R^{\text{vis}}\right\}. \tag{1}$$

It is a round region centered in $\mathbf{x}_i(t)$ with radius R^{vis}, i.e., represents a vision depth which is hereafter set equal to 10 m according to the characteristic dimensions of swarm migration considered in this work.

2.2. Bee dynamics

The dynamics of a generic bee i can be described starting from a general second-order particle model:

$$m_i \frac{d^2\mathbf{x}_i}{dt^2}(t) + \lambda_i \frac{d\mathbf{x}_i}{dt}(t) = \mathbf{F}_i(t), \tag{2}$$

where m_i is the individual mass and λ_i a friction coefficient. $\mathbf{F}_i$ denotes instead the resultant of the forces that affect insect behavior. However, it is worth to notice that bees (such as most living entities, e.g., from cells and bacteria to big animal species and humans) are not passively prone to the Newtonian laws of inertia. They are in fact intelligent individuals able to actively develop behavioral strategies, which depend both on intrinsic stimuli and on the interactions with the surrounding environment. For instance, bees can control their movement without undergoing inertial effects: in other words, they can suddenly decide to stop and change direction of motion, at least for reasonable speeds. These concepts allow to neglect the inertial term in Eq. (2), i.e., to assume, in mathematical terms, that $\lambda_i >> m_i$ and to obtain

$$\underbrace{\frac{m_i}{\lambda_i}}_{\to 0} \frac{d^2\mathbf{x}_i}{dt^2}(t) + \frac{d\mathbf{x}_i}{dt}(t) = \frac{\mathbf{F}_i(t)}{\lambda_i} \qquad \Rightarrow \qquad \frac{d\mathbf{x}_i}{dt}(t) = \frac{\mathbf{F}_i(t)}{\lambda_i} = \underbrace{\widetilde{\mathbf{v}}_i(t)}_{\substack{\text{bee} \\ \text{velocity}}}. \tag{3}$$

Eq. (3) gives the so-called *overdamped force-velocity response* relation, which states that the velocity of an individual, and not his/her acceleration, is proportional to the acting forces: it is employed in a number of discrete/IBM approaches (see [14], [19], [27] and [41] and references therein for comments) and allows to describe selected bee behavior by a direct phenomenological postulation of the velocity contributions, i.e., by a first-order model.

The individual velocity $\widetilde{\mathbf{v}}_i$ has then to be characterized by a realistic modulus, which has to be subjected to physical constraints and limitations. In this respect, the equation of motion of the generic bee i (with $i = 1, ..., N$) is finally assumed to be

$$\frac{d\mathbf{x}_i(t)}{dt} = \widetilde{\mathbf{v}}_i(t) = \underbrace{\min\left\{v_{\max}, |\mathbf{v}_i(t)|\right\}}_{\text{speed control}} \frac{\mathbf{v}_i(t)}{|\mathbf{v}_i(t)|} \tag{4}$$

In Eq. (4), $v_{\max}$ is indeed a maximal speed characteristic of flying bees: it is set equal to 9.4 m/s [42] and allows to consistently control the modulus of individual velocities.

To completely determine the behavior of the population of bees, we have then to phenomenologically specify the individual velocity. In this respect, we take into account and enrich the set of basic rules called the "first sociological principles of swarming" [9], i.e., for each insect i we define:

$$\mathbf{v}_i(t) = \underbrace{\mathbf{v}_i^{\text{targ}}(t)}_{\text{individual strategy}} + \underbrace{\mathbf{v}_i^{\text{soc}}(t)}_{\text{social interactions}} + \underbrace{\xi_i^{\text{fluct}}(t)}_{\text{noise}}. \tag{5}$$

The first term in Eq. (5) describes the attempt of a bee to reach a target destination while minimizing the effort, e.g., to cover the shortest possible path at a comfort speed (other strategic behavior may of course be taken into account). The third velocity contribution is a random fluctuation term, that implements the impossibility of an individual to apply the ideal set of rules, e.g., to take the correct and productive decision in a very short time. Finally, the social velocity contribution $\mathbf{v}_i^{\text{soc}}$ includes different individual behaviors:

$$\mathbf{v}_i^{\text{soc}}(t) = \mathbf{v}_i^{\text{rep}}(t) + \mathbf{v}_i^{\text{attr}}(t) + \mathbf{v}_i^{\text{align}}(t). \tag{6}$$

The repulsive component $\mathbf{v}_i^{\text{rep}}$ models the tendency of the generic i-th bee of staying sufficiently far away from its neighbours, typically in order to avoid physical collisions, while maintaining a minimal comfort space within the swarm. The second contribution in Eq. (6) implements the desire of each individual to keep a connection with the groupmates, i.e., to be close enough to the rest of the population. Finally, the third social velocity contribution describes the alignment process of bees, i.e., the adaptation and synchronization of their movement with at least a given part of the swarm.

Entering in more details, the repulsive/attractive behavior of the i-th bee is described by proper kernels $\mathbf{H}_{ij}^{\text{rep}}, \mathbf{H}_{ij}^{\text{attr}} : \mathbb{R}^2 \times \mathbb{R}^2 \longmapsto \mathbb{R}^2$, which define its pairwise interaction instances with the generic j-th individual falling within a given surrounding region, say Ω_i^{rep} or Ω_i^{attr}, respectively. We then assume that the above-introduced kernels do not depend on the specific couple of bees, i.e., $\mathbf{H}_{ij}^{\text{rep}} = \mathbf{H}^{\text{rep}}$ and $\mathbf{H}_{ij}^{\text{attr}} = \mathbf{H}^{\text{attr}}$ for any (i, j), that the resulting velocity contributions have an effect on the direction ideally connecting the interacting insects and finally that they depend on individual relative dis-

tance. In this respect, we can write:

$$\begin{aligned}\mathbf{v}_i^{\text{rep}}(t) &= \sum_{j\in\Omega_i^{\text{rep}}(t)} \mathbf{H}^{\text{rep}}(\mathbf{x}_j(t),\mathbf{x}_i(t)) \\ &= \sum_{j\in\Omega_i^{\text{rep}}(t)} h^{\text{rep}}(|\mathbf{x}_j(t)-\mathbf{x}_i(t)|)\frac{\mathbf{x}_j(t)-\mathbf{x}_i(t)}{|\mathbf{x}_j(t)-\mathbf{x}_i(t)|};\end{aligned} \tag{7}$$

$$\begin{aligned}\mathbf{v}_i^{\text{attr}}(t) &= \sum_{j\in\Omega_i^{\text{attr}}(t)} \mathbf{H}^{\text{attr}}(\mathbf{x}_j(t),\mathbf{x}_i(t)) \\ &= \sum_{j\in\Omega_i^{\text{attr}}(t)} h^{\text{attr}}(|\mathbf{x}_j(t)-\mathbf{x}_i(t)|)\frac{\mathbf{x}_j(t)-\mathbf{x}_i(t)}{|\mathbf{x}_j(t)-\mathbf{x}_i(t)|},\end{aligned} \tag{8}$$

where the continuous and Lebesgue integrable functions $h^{\text{rep}}, h^{\text{attr}} : \mathbb{R}_+ \longmapsto \mathbb{R}$ are such that

$$h^{\text{rep}}(|\mathbf{x}_j(t)-\mathbf{x}_i(t)|) \leq 0; \tag{9}$$

$$h^{\text{attr}}(|\mathbf{x}_j(t)-\mathbf{x}_i(t)|) \geq 0, \tag{10}$$

for all pairs of bees (i,j) and corresponding positions $(\mathbf{x}_i, \mathbf{x}_j)$. The combination of attractive/repulsive mechanisms has to assure that the swarm does not collapse nor unrealistically explode. Rather, the component bees have to find an optimal spacing during motion, as experimentally observed [42]. In this respect, previous works [9], [22] showed that a particle system reaches and maintains a *crystalline*-like configuration, i.e., a configuration characterized by a finite, strictly positive, minimal interparticle distance regardless of the number of component agents, if the relative individual interaction potential is *H-stable* in the sense of statistical mechanics [39]. In the following, taking advantage of the analytical study in [4], which has been recently applied for the first time to the case of cell aggregates in [6], we will indeed give a set of conditions both on the form of h^{rep} and h^{attr} and on the corresponding characteristic parameters that will certainly result in realistic, H-stable, bee patterns.

The alignment contribution in the dynamics of the generic i-th bee results instead from a mean over the velocity of a given set of its neighbours, i.e.,

$$\mathbf{v}_i^{\text{align}}(t) = < \mathbf{v}_j(t) >_{j\in\Omega_i^{\text{aling}}(t)} . \tag{11}$$

The specification of each social velocity component, as well as the definition of the corresponding set of interacting particles, results in different models of

Table 1: Model parameters and corresponding references.

Parameter	Description	Value [Unit]	Reference
R^{vis}	bee visual depth	10 [m]	estimated
R^{rep}	repulsion range	0.3 [m]	[42]
R^{attr}	attraction range	10 [m]	estimated
$v_{\max}$	bee maximal speed	9.4 [m/s]	[42]
N	number of bees	100	

bee collective behavior. In this respect, in the next sections, we will propose different hypothesis on the alignment mechanism, which impact also on the expression of the other terms included in Eq. (6).

3. Social velocity components: Assumptions and corresponding simulations

3.1. Euclidean metric-based alignment mechanism

We first assume that the alignment mechanism, as well as the individual repulsive/attractive behavior, relies on Euclidean metric arguments, i.e., for any $i = 1, \dots, N$, it involves all the bees $j = 1, \dots, N$, with $i \neq j$, whose distance from the i-th insect falls within a given range. In particular, we identify three concentric regions such that each of them characterizes one of the social velocity components (see Fig. 2, left panel):

$$\Omega_i^{\text{rep}}(t) = \left\{\mathbf{x} \in \Omega_i^{\text{vis}}(t) : 0 < |\mathbf{x} - \mathbf{x}_i(t)| \leq R^{\text{rep}}\right\}; \tag{12}$$

$$\Omega_i^{\text{align}}(t) = \left\{\mathbf{x} \in \Omega_i^{\text{vis}}(t) : R^{\text{rep}} < |\mathbf{x} - \mathbf{x}_i(t)| \leq R^{\text{align}}\right\}; \tag{13}$$

$$\Omega_i^{\text{attr}}(t) = \left\{\mathbf{x} \in \Omega_i^{\text{vis}}(t) : R^{\text{align}} < |\mathbf{x} - \mathbf{x}_i(t)| \leq R^{\text{attr}}\right\}, \tag{14}$$

where Ω_i^{vis} is the actual visual field of the i-th bee, as defined in Eq. (1). In this perspective, in Eqs. (7), (8), and (11), the notation $j \in \Omega_i^{\bullet}(t)$ has to be intended as $j : \mathbf{x}_j(t) \in \Omega_i^{\bullet}(t)$, where $\bullet \in \{\text{“rep”}, \text{“attr”}, \text{“align”}\}$.

To completely determine individual dynamics, we have finally to define the interaction kernels. In this respect, although there are several possible options, we take advantage of some published results [12], [13] and set, for

each couple of bees (i, j):

$$h^{\text{rep}}(r) = \begin{cases} F^{\text{rep}} \left(\dfrac{1}{R^{\text{rep}}} - \dfrac{1}{r} \right), & \text{if } 0 < r \leq R^{\text{rep}}; \\ 0, & \text{otherwise;} \end{cases} \tag{15}$$

$$h^{\text{attr}}(r) = \begin{cases} -\dfrac{4\, F^{\text{attr}}\, (r - R^{\text{attr}})\, (r - R^{\text{align}})}{(R^{\text{attr}} - R^{\text{align}})^2}, & \text{if } R^{\text{align}} < r \leq R^{\text{attr}} \\ 0, & \text{otherwise.} \end{cases} \tag{16}$$

The functions defined in Eqs. (15)-(16), and plotted in Fig. 2 (right panel), are intrinsically multiparametric, since they are characterized by the following set of coefficients:

$$(R^{\text{rep}}, R^{\text{align}}, R^{\text{attr}}, F^{\text{rep}}, F^{\text{attr}}) \in \mathbb{R}^5_+.$$

To decrease the complexity of the problem, we can reduce the dimension of the free parameter space with phenomenological arguments and observations. First of all, R^{rep} can be intended as the comfort distance that each bee tends to preserve in order to fly without colliding with other components of the swarm. According to several experimental measurements, we estimate $R^{\text{rep}} = 0.3$ m [42]. On the opposite, R^{attr} is the extension of the long-range attraction, i.e., of the desire of each individual to remain sufficiently close to the rest of the population. In this respect, it is consistent to assume $R^{\text{attr}} = R^{\text{vis}} = 10$ m, i.e., each bee is attracted by the groupmates that it is able to see (and that do not fall within the alignment and repulsion regions). In this respect, given the estimated extension of the three interaction neighborhoods, we have that

$$\Omega_i^{\text{rep}}(t) \cup \Omega_i^{\text{align}}(t) \cup \Omega_i^{\text{attr}}(t) = \Omega_i^{\text{vis}}(t),$$

for each insect i and time t, see again Fig. 2 (left panel).

The above considerations allow us to reduce the parameter space of the problem to

$$(R^{\text{align}}, F^{\text{rep}}, F^{\text{attr}}) \in [R^{\text{rep}}, R^{\text{attr}}] \times \mathbb{R}^2_+.$$

Given the form of $h^{\text{attr}}(r)$, $F^{\text{attr}} \in [0, v_{\max}]$ can be interpreted as the maximal attraction speed, whereas $F^{\text{rep}} > 0$ determines the slope of the hyperbolic part of $h^{\text{rep}}(r)$ (cf. Fig. 2, right panel).

Further, the swarm has to maintain a realistic crystalline configuration during the collective flight. In this respect, it has been shown that the large-time asymptotic collective pattern of discrete particle systems depends on

the stability characteristics of the potential relative to individual pairwise interactions [39]. In particular, we use and extend to our case the criterium introduced in [4], recently applied to the case of cell aggregates in [6], in order to identify the regions of the free parameter space that assure the H-stability of a particle system. We can indeed prove:

Theorem 3.1. *If the following parametric relation*

$$\frac{F^{\mathrm{rep}}}{F^{\mathrm{attr}}} > \frac{2(R^{\mathrm{attr}} - R^{\mathrm{align}})}{5(R^{\mathrm{rep}})^2} \left(3(R^{\mathrm{align}})^2 + 4R^{\mathrm{attr}}R^{\mathrm{align}} + 3(R^{\mathrm{attr}})^2\right) \tag{17}$$

holds, the potential related to the pairwise interaction kernel $h^{\mathrm{int}}(r) = h^{\mathrm{rep}}(r) + h^{\mathrm{attr}}(r)$*, with* $r = |\boldsymbol{x}_i(t) - \boldsymbol{x}_j(t)|$*, defined in Eqs. (15)-(16) is H-stable. As shown in [4], [9], [22], for a finite number of agents, as in the case of our interest, this implies that, at each time* $t \in R_+$*, there exist two finite and positive quantities* $d_{\min}(t) = \min_{\substack{(i,j)\in\{1,\dots,N\} \\ i\neq j}} |\boldsymbol{x}_i(t) - \boldsymbol{x}_j(t)|$ *and* $D_{\max}(t) = \max_{\substack{(i,j)\in\{1,\dots,N\} \\ i\neq j}} |\boldsymbol{x}_i(t) - \boldsymbol{x}_j(t)|$ *such that* $d_{\min}(t) \leq |\boldsymbol{x}_i(t) - \boldsymbol{x}_j(t)| \leq D_{\max}(t)$ *for all pairs* (i, j) *of bees, i.e., at each time* $t \in R_+$ *the swarm does not collapse nor explode. In particular, for* $t \to +\infty$*, the minimal relative distance between bees* $d_{\min}(t)$ *tends to the limit value* d_∞*, whereas the maximal relative distance* $D_{\max}(t)$ *(which also represents the diameter of the swarm) tends to the value* D_∞*: in other words, the particle population asymptotically organizes in a stable crystalline-like pattern.*

Proof. Following the analytical study in [4] and the calculations introduced in [6], we have first to define a potential $u^{\mathrm{int}} : R \longmapsto R$ associated to our

pairwise interaction kernels, i.e.,

$$u^{\rm int}(r) = \int h^{\rm int}(r)dr = \int h^{\rm rep}(r)dr + \int h^{\rm attr}(r)dr =$$

$$= \begin{cases} F^{\rm rep}\left(\dfrac{r}{R^{\rm rep}} - \log r\right) + C_1, \\ \text{if } 0 < r \leq R^{\rm rep}; \\ \\ C_2, \\ \text{if } R^{\rm rep} < r \leq R^{\rm align}; \\ \\ -\dfrac{2\,F^{\rm attr}\left(2\,r^3 - 3\,(R^{\rm attr} + R^{\rm align})\,r^2 + 6\,R^{\rm attr}\,R^{\rm align}\,r\right)}{3(R^{\rm attr} - R^{\rm align})^2} + C_3, \\ \text{if } R^{\rm align} < r \leq R^{\rm attr}; \\ \\ C_4, \\ \text{otherwise,} \end{cases}$$

where the constants C_1, C_2, C_3, C_4 have to satisfy the following conditions

$$\begin{cases} C_1 = C_2 - F^{\rm rep}\,(1 - \log R^{\rm rep})\,; \\ \\ C_2 = C_3 - \dfrac{2\,F^{\rm attr}\left(2\,(R^{\rm align})^3 - 3\,(R^{\rm attr} + R^{\rm align})\,(R^{\rm align})^2 + 6\,R^{\rm attr}\,(R^{\rm align})^2\right)}{3\,(R^{\rm attr} - R^{\rm align})^2}; \\ \\ C_3 = C_4 + \dfrac{2\,F^{\rm attr}\left(2\,(R^{\rm attr})^3 - 3\,(R^{\rm attr} + R^{\rm align})\,(R^{\rm attr})^2 + 6\,(R^{\rm attr})^2\,R^{\rm align}\right)}{3\,(R^{\rm attr} - R^{\rm align})^2}, \end{cases}$$

to assure its continuity. To fully apply the characterization of H-stable potentials given in [4], $u^{\rm int}$ has to be essentially negligible for large interparticle distances (i.e., $\lim\limits_{r\to\infty} u^{\rm int}(r) = 0$). Without loss of generality, we indeed assume $C_4 = 0$. As a consequence, with simple algebraic calculations, we have that

$$\begin{cases} C_3 = -\dfrac{2\,F^{\rm attr}(R^{\rm attr})^2\left(R^{\rm attr} - 3\,R^{\rm align}\right)}{3\,(R^{\rm attr} - R^{\rm align})^2}; \\ \\ C_2 = -\dfrac{2}{3}\,F^{\rm attr}\,(R^{\rm attr} - R^{\rm align}); \\ \\ C_1 = -\dfrac{2}{3}\,F^{\rm attr}\,(R^{\rm attr} - R^{\rm align}) - F^{\rm rep}\,(1 - \log R^{\rm rep})\,. \end{cases}$$

The pairwise interaction potential therefore rewrites in the following explicit form

$$u^{\text{int}}(r) = \begin{cases} F^{\text{rep}}\left(\dfrac{r}{R^{\text{rep}}} - \log\left(\dfrac{r}{R^{\text{rep}}}\right) - 1\right) - \dfrac{2}{3}F^{\text{attr}}\,(R^{\text{attr}} - R^{\text{align}}), \\ \text{if } 0 < r \leq R^{\text{rep}}; \\ \\ -\dfrac{2}{3}F^{\text{attr}}\,(R^{\text{attr}} - R^{\text{align}}), \\ \text{if } R^{\text{rep}} < r \leq R^{\text{align}}; \\ \\ -\dfrac{2\,F^{\text{attr}}\left(2r^3 - 3(R^{\text{attr}} + R^{\text{align}})r^2 + 6R^{\text{attr}}R^{\text{align}}r + (R^{\text{attr}})^2\left(R^{\text{attr}} - 3R^{\text{align}}\right)\right)}{3(R^{\text{attr}} - R^{\text{align}})^2}, \\ \text{if } R^{\text{align}} < r \leq R^{\text{attr}}; \\ \\ 0, \\ \text{otherwise.} \end{cases} \tag{18}$$

Now, recalling the Definition 1.1 in [4], we can say that u^{int} (and consequently h^{int}) is H-stable if

$$\int_0^{+\infty} u^{\text{int}}(r)\,r\,dr > \frac{1}{2}\lim_{r\to+\infty} u^{\text{int}}(r) = 0.$$

In this respect, let us calculate the value of the integral of interest:

$$\begin{aligned} &\int_0^{+\infty} u^{\text{int}}(r) r\,dr \;= \\ &= \int_0^{R^{\text{rep}}} \left(F^{\text{rep}}\left(\frac{r^2}{R^{\text{rep}}} - r\log\left(\frac{r}{R^{\text{rep}}}\right) - r\right) - \frac{2}{3}F^{\text{attr}}(R^{\text{attr}} - R^{\text{align}})r\right) dr \\ &\quad - \int_{R^{\text{rep}}}^{R^{\text{align}}} \left(\frac{2}{3}F^{\text{attr}}(R^{\text{attr}} - R^{\text{align}})r\right) dr \\ &\quad - \int_{R^{\text{align}}}^{R^{\text{attr}}} \left(\frac{2F^{\text{attr}}\left(2r^4 - 3(R^{\text{attr}} + R^{\text{align}})r^3 + 6R^{\text{attr}}R^{\text{align}}r^2 + (R^{\text{attr}})^2\left(R^{\text{attr}} - 3R^{\text{align}}\right)r\right)}{3(R^{\text{attr}} - R^{\text{align}})^2}\right) dr \\ &= \frac{F^{\text{rep}}(R^{\text{rep}})^2}{12} - \frac{F^{\text{attr}}}{30}(R^{\text{attr}} - R^{\text{align}})\Big(3(R^{\text{align}})^2 + 4R^{\text{attr}}R^{\text{align}} + 3(R^{\text{attr}})^2\Big), \end{aligned}$$

which is non-negative (assuring indeed the H-stability of the system) if the parametric relation in Eq. (17) holds.

Theorem 3.1 allows to better identify the parameter space, that is drawn in Fig. 3 (for the sake of clarity, we recall that $R^{\rm attr} = 10$ m and that $R^{\rm rep} = 0.3$ m). Specifically, only the points above the plotted surface are able to satisfy both the experimental observations and the relation (17) (that assure the H-stability of the system). Each point of this area leads, in principle, to a different system evolution.

In this respect, we now turn to analyze swarm dynamics upon permitted variations of the model coefficients, i.e., within the region of H-stability. In particular, we study the behavior of a population formed by $N = 100$ bees. The swarm is initially arranged in an almost round pattern of radius equal to 2 m and centered at $(2.5 \text{ m}, 2.5 \text{ m})$, i.e., we initially account for a reasonable density of ≈ 8 bees/m^2 [42] (see Fig. 4, left panel). The group of insects behaves following the system (4). In particular we set:

$$\mathbf{v}_1(t) = \mathbf{v}_1^{\rm targ}(t) + \mathbf{v}_1^{\rm rep}(t) + \mathbf{v}_1^{\rm attr}(t); \tag{19}$$

$$\mathbf{v}_i(t) = \mathbf{v}_i^{\rm rep}(t) + \mathbf{v}_i^{\rm attr}(t) + \mathbf{v}_i^{\rm align}(t), \qquad \forall\ i = 2, ..., N. \tag{20}$$

With the phenomenological rules given in Eqs. (19)-(20), we are assuming that all bees are characterized by repulsive/attractive interactions, which are given in Eqs. (15)-(16). Further, only one bee, identified with the index 1, is set to have a target velocity component, i.e., it is the only one *informed* of the destination of the entire swarm (e.g., of the presence of a possible nest). On the opposite, all the other individuals undergo alignment process, which is defined in Eq. (11) and allows a flight synchronization within the insect population. The presence of a small group of leader bees within a swarm, which are able to guide the rest of the population is widely known from the ecological literature [42]. Entering in more details, assuming $\mathbf{x}_{\rm d} = (10 \text{ m}, 2.5$ m) as the target point (e.g., the location of the nest), we set

$$\mathbf{v}_1^{\rm targ}(t) = v_{\max} \frac{\mathbf{x}_{\rm d} - \mathbf{x}_i(t)}{|\mathbf{x}_{\rm d} - \mathbf{x}_i(t)|}, \tag{21}$$

i.e., the leader bee aims to cover the shortest possible path towards the destination at the maximal speed. Further, we do not consider fluctuation terms in the problem. The parameter values used in the simulations are summarized in Table 1. Finally, we introduce the following classification of the particle system evolution:

Definition 3.1. *The population of uninformed bees has a time asymptotic collective swarming behavior (with respect to the informed individual) if the following condition is satisfied:*

$$\lim_{t\to\infty} V_{\text{swarm}}(t) = \lim_{t\to\infty} \sqrt{\sum_{i=2}^{N} |\boldsymbol{v}_i(t) - \boldsymbol{v}_1(t)|^2} = 0. \tag{22}$$

The swarm undergoes a collective productive motion if the following condition is satisfied:

$$\lim_{t\to\infty} X_{\text{swarm}}(t) = \lim_{t\to\infty} \left| \frac{\sum_{i=2}^{N} \boldsymbol{x}_i(t)}{N-1} - \boldsymbol{x}_{\text{d}} \right| = 0, \tag{23}$$

i.e., if the population of uninformed individuals (in terms of barycenter displacement) approaches the target destination. Representative sketches of the distinct behavior of the bee population are given in Figs. 5 - 6.

Among the possible combinations of the free model parameters R^{align}, F^{rep}, and F^{attr}, resulting both from experimental considerations and from the H-stability criterium, we hereafter focus on six representative sets, which are indicated in Fig. 3 by the points Mk (where $k = 1, ..., 6$): they are in fact sufficiently distributed and allow the classification of swarm dynamics in large enough parameter regimes.

We first observe that in all cases the swarm organizes in a crystalline-like configuration: as shown in Fig. 7, d_{min}, i.e., the measure of the distance between pairs of first closest bees, in fact quickly stabilizes to the asymptotic threshold $d_\infty = 0.3$ m, which results in a overall swarm diameter of about $D_\infty = 3.75$ m. Such values are consistent with R_{rep}, i.e., the approximate extension of the comfort space that each insect desires to maintain during its flight, as commented in the experimental literature [42]. In this respect, we further observe that increments in F^{rep} result in increments in the time needed to the particle system to reach the stable configuration (see, for instance, the cases $M1$ and $M2$ in Fig. 7). This behavior, which is independent from the specific value of the other model parameters, is due to the enhanced role of the repulsive force which, at the initial stages of the system evolution, i.e., when the bee cloud is more compact, overcomes the other velocity contributions, pushing away the insects one from each other and therefore delaying the achievement of a stable pattern. In this respect, we remark that the obtained asymptotic crystalline configuration of the swarm is consistent

with, and predicted by, the analytical results of Theorem 3.1, given that the sets of parameter values employed in this series of simulations satisfy relation (17), which assures the H-stability of the pairwise interaction kernels and therefore of the overall particle system.

We then turn to analyze the migratory determinants of the swarm. From Fig. 8, it is possible to observe that, regardless of the values of F^{rep} and F^{attr}, the bee cloud undergoes swarming with productive motion (i.e., towards the target destination) only if the extension of the alignment region, i.e., R^{align}, is sufficiently large (see the parameter settings $M1$, $M2$, $M5$, and $M6$). Otherwise, the insect cloud is characterized by uncorrelated individual movement (see the parameter settings $M3$ and $M4$). Entering in more details, let us compare Figs. 7 and 8: it is straightforward to notice that the flight synchronization process starts at $t \approx 0.01$, i.e., just after the stabilization of the bee configuration. In this perspective, our simulations point out that a value of R^{align} not smaller than the asymptotic diameter of the insect cloud $D_\infty = 3.75$ is needed to have swarming and productive motion, i.e., it is necessary that each bee has, at the same time, almost the rest of the groupmates (included the leader) within its flight synchronization region.

We can indeed conclude that, under our first hypothesis on the alignment process, the swarm is characterized by two-step dynamics: in the fist stages, the bee cloud organizes in a crystalline configuration (regardless of the parameter values, provided the H-stability condition); in the later phases, if R^{align} is large enough (i.e., $\geq D_\infty$), the component insects synchronize their velocity and the overall population undergoes productive directional movement.

3.2. Topological neighborhood metric-based alignment mechanism

In our second hypothesis, the alignment mechanism of bees involves a topological neighborhood metric. In more details, the i-th insect tracks and synchronizes its movement with the a-th seen closest individuals, regardless of their position, and not with all (or only) the individuals placed within a given alignment region. In this respect, we set

$$\Omega_i^{\text{align}}(t) = \left\{ j : \mathbf{x}_j(t) \in \Omega_i^{\text{vis}}(t) \text{ and } j \text{ is one of the } a\text{-th closest neighbors of } i \right\}, \tag{24}$$

where a can be interpreted as a sort of interindividual *communication rate*.

On the opposite, the repulsive/attractive velocity components still rely on an Euclidean metric, i.e., they involve the couples of bees whose relative

distance falls within a given range. In particular, the interaction regions slightly differ from the previous case (see Fig. 9, left panel):

$$\Omega_i^{\rm rep}(t) = \left\{\mathbf{x} \in \Omega_i^{\rm vis}(t) : 0 < |\mathbf{x} - \mathbf{x}_i(t)| \leq R^{\rm rep}\right\}; \tag{25}$$

$$\Omega_i^{\rm attr}(t) = \left\{\mathbf{x} \in \Omega_i^{\rm vis}(t) : R^{\rm rep} < |\mathbf{x} - \mathbf{x}_i(t)| \leq R^{\rm attr}\right\}. \tag{26}$$

The interaction kernels, in particular the adhesive part, have then to adapt to the new hypothesis as well (see Fig. 9, right panel):

$$h^{\rm rep}(r) = \begin{cases} F^{\rm rep}\left(\dfrac{1}{R^{\rm rep}} - \dfrac{1}{r}\right), & \text{if } 0 < r \leq R^{\rm rep}; \\ 0, & \text{otherwise;} \end{cases} \tag{27}$$

$$h^{\rm attr}(r) = \begin{cases} -\dfrac{4F^{\rm attr}\,(r - R^{\rm attr})\,(r - R^{\rm rep})}{(R^{\rm attr} - R^{\rm rep})^2}, & \text{if } R^{\rm rep} < r \leq R^{\rm attr}; \\ 0, & \text{otherwise,} \end{cases} \tag{28}$$

where again $R^{\rm rep} = 0.3$ m and $R^{\rm attr} = R^{\rm vis} = 10$ m. In this respect, in this case we have that $\Omega_i^{\rm rep}(t) \cup \Omega_i^{\rm attr}(t) = \Omega_i^{\rm vis}(t)$ for each insect i and time t.

Remark We underline that, according to our second hypothesis, the social behavior of a bee can *simultaneously* involve alignment and attractive (or repulsive) stimuli due to the presence of the same groupmate. On the opposite, in the case of our first hypothesis, the j-th animal was only permitted to affect one of the social velocity contributions of the i-insect (i.e., j could fall within only one of the interaction regions of i), compare Figs. 2 and 9 (left panels).

According to the second type of assumptions, the space of free parameters regulating bee dynamics now reads as

$$(F^{\rm rep}, F^{\rm attr}, a),$$

where $F^{\rm rep} \in R_+$, $F^{\rm attr} \in [0, v_{\max}]$, and $a \in \{1, ..., N-1\}$, being N the total number of insects. In this respect, the assumption of H-stability of the system allows to have a functional relation between the coefficients $F^{\rm rep}$ and $F^{\rm attr}$, as stated by the following

Theorem 3.2. *If the following parametric relation*

$$\frac{F^{\rm rep}}{F^{\rm attr}} > \frac{2(R^{\rm attr}-R^{\rm rep})}{5(R^{\rm rep})^2}\left(3(R^{\rm rep})^2+4R^{\rm attr}R^{\rm rep}+3(R^{\rm attr})^2\right) \qquad (29)$$

holds, the potential related to the pairwise interaction kernel $h^{\rm int}(r)=h^{\rm rep}(r)+h^{\rm attr}(r)$*, with* $r=|\boldsymbol{x}_i(t)-\boldsymbol{x}_j(t)|$*, defined in Eqs. (15)-(16) is H-stable. As shown in [4], [9], [22], for a finite number of agents, as in the case of our interest, this implies that, at each time* $t\in R_+$*, there exist two finite and positive quantities* $d_{\min}(t)=\min\limits_{\substack{(i,j)\in\{1,\dots,N\}\\ i\neq j}}|\boldsymbol{x}_i(t)-\boldsymbol{x}_j(t)|$ *and* $D_{\max}(t)=\max\limits_{\substack{(i,j)\in\{1,\dots,N\}\\ i\neq j}}|\boldsymbol{x}_i(t)-\boldsymbol{x}_j(t)|$ *such that* $d_{\min}(t)\leq|\boldsymbol{x}_i(t)-\boldsymbol{x}_j(t)|\leq D_{\max}(t)$ *for all pairs* (i,j) *of bees, i.e., at each time* $t\in R_+$ *the swarm does not collapse nor explode. In particular, for* $t\to+\infty$*, the minimal relative distance between bees* $d_{\min}(t)$ *tends to the limit value* d_∞*, whereas the maximal relative distance* $D_{\max}(t)$ *(which also represents the diameter of the swarm) tends to the value* D_∞*: in other words, the particle population asymptotically organizes in a stable crystalline-like pattern.*

Proof. The proof closely resembles the one of Theorem 3.1 which, as already explained, relies on the analytical study in [4] and on the calculations firstly introduced in [6] to the case of cell aggregates. Entering in more details, the potential $u^{\rm int}: R\longmapsto R$ associated to the pairwise interaction kernels defined in (27)-(28) has the form

$$u^{\rm int}(r) = \int h^{\rm int}(r)dr=\int h^{\rm rep}(r)dr+\int h^{\rm attr}(r)dr=$$

$$=\begin{cases} F^{\rm rep}\left(\dfrac{r}{R^{\rm rep}}-\log r\right)+A_1, \\ \text{if } 0<r\leq R^{\rm rep}; \\ \\ -\dfrac{2\,F^{\rm attr}\,(2\,r^3-3\,(R^{\rm attr}+R^{\rm rep})\,r^2+6\,R^{\rm attr}\,R^{\rm rep}\,r)}{3(R^{\rm attr}-R^{\rm rep})^2}+A_2, \\ \text{if } R^{\rm rep}<r\leq R^{\rm attr}; \\ \\ A_3, \\ \text{otherwise,} \end{cases}$$

where the constants A_1, A_2, A_3 have to satisfy the following conditions

$$\begin{cases} A_1 &= A_2 - \dfrac{2F^{\rm attr}\,(2(R^{\rm rep})^3 - 3(R^{\rm attr}+R^{\rm rep})(R^{\rm rep})^2 + 6R^{\rm attr}(R^{\rm rep})^2)}{3(R^{\rm attr}-R^{\rm rep})^2} \\ &- F^{\rm rep}(1-\log R^{\rm rep}); \\ \\ A_2 &= A_3 + \dfrac{2F^{\rm attr}\,(2(R^{\rm attr})^3 - 3(R^{\rm attr}+R^{\rm rep})(R^{\rm attr})^2 + 6(R^{\rm attr})^2R^{\rm rep})}{3(R^{\rm attr}-R^{\rm rep})^2}, \end{cases}$$

to assure its continuity. As done for Theorem 3.1, let us now assume that $u^{\rm int}(r) \to 0$ when $r \to \infty$ and set $A_3 = 0$. We have indeed that

$$\begin{cases} A_2 &= -\dfrac{2F^{\rm attr}(R^{\rm attr})^2\,(R^{\rm attr}-3R^{\rm rep})}{3(R^{\rm attr}-R^{\rm rep})^2}; \\ \\ A_1 &= -\dfrac{2}{3}\,F^{\rm attr}(R^{\rm attr}-R^{\rm rep}) - F^{\rm rep}(1-\log R^{\rm rep}). \end{cases}$$

The particle interaction potential is therefore given by

$$u^{\rm int}(r) = \begin{cases} F^{\rm rep}\left(\dfrac{r}{R^{\rm rep}} - \log\left(\dfrac{r}{R^{\rm rep}}\right) - 1\right) - \dfrac{2}{3}\,F^{\rm attr}\,(R^{\rm attr}-R^{\rm rep}), \\ \text{if } 0 < r \le R^{\rm rep}; \\ \\ -\dfrac{2\,F^{\rm attr}\,(2r^3 - 3(R^{\rm attr}+R^{\rm rep})r^2 + 6R^{\rm attr}R^{\rm rep}r + (R^{\rm attr})^2\,(R^{\rm attr}-3R^{\rm rep}))}{3(R^{\rm attr}-R^{\rm rep})^2}, \\ \text{if } R^{\rm rep} < r \le R^{\rm attr}; \\ \\ 0, \\ \text{otherwise.} \end{cases} \tag{30}$$

Recalling again the criterium given in [4], the potential $u^{\rm int}$ defined in (30) is H-stable if the already-introduced relation $\int_0^{+\infty} u^{\rm int}(r)\,r\,dr > 0$ holds. In

this respect, let us calculate

$$\begin{aligned}
&\int_0^{+\infty} u^{\text{int}}(r) r\, dr \;=\\
&= \int_0^{R^{\text{rep}}} \left(F^{\text{rep}} \left(\frac{r^2}{R^{\text{rep}}} - r \log\left(\frac{r}{R^{\text{rep}}}\right) - r \right) - \frac{2}{3} F^{\text{attr}} (R^{\text{attr}} - R^{\text{rep}}) r \right) dr +\\
&\quad - \int_{R^{\text{rep}}}^{R^{\text{attr}}} \left(\frac{2F^{\text{attr}} \left(2r^4 - 3(R^{\text{attr}} + R^{\text{rep}}) r^3 + 6R^{\text{attr}} R^{\text{rep}} r^2 + (R^{\text{attr}})^2 \left(R^{\text{attr}} - 3R^{\text{rep}}\right) r\right)}{3(R^{\text{attr}} - R^{\text{rep}})^2} \right) dr\\
&= \frac{F^{\text{rep}} (R^{\text{rep}})^2}{12} - \frac{F^{\text{attr}}}{30} (R^{\text{attr}} - R^{\text{rep}}) \Big(3(R^{\text{rep}})^2 + 4R^{\text{attr}} R^{\text{rep}} + 3(R^{\text{attr}})^2 \Big),
\end{aligned}$$

which is non-negative (assuring indeed the H-stability of the system) if the parametric relation defined in Eq. (29) is satisfied.

With respect to Theorem 3.1, the criterium given in (29) involves only F^{rep} and F^{attr} and not the third free model coefficient a, which can instead independently vary without affecting the H-stability of the system (recalling that $R^{\text{rep}} = 0.3$ m and $R^{\text{attr}} = 10$ m, the permitted region of the parameter space is represented in Fig. 10). As in the previous section, we then focus on the swarm behavior in selected parameter settings, labeled by Tk, where $k = 1, ..., 5$, and chosen to span the entire region of interest of the coefficient values. In particular, in the following numerical realizations, we maintain the domain configuration, as well as the initial conditions and the differentiated bee behavior (i.e., a leader insect which guides the rest of uninformed individuals), of the simulation proposed in the previous section (see Fig. 4). The only modification is that the social velocity components are now determined by the interaction sets introduced in Eqs. (24)-(25)-(26) while the repulsive/attractive dynamics are defined in Eqs. (27)-(28). Also in this case, we neglect a random contribution in bee behavior, whereas the parameter values used in the simulations can be found in Table 1. The resulting swarm dynamics are classified according to Definition 3.1.

As shown in Fig. 11, we observe that the swarm constantly reaches a stable crystalline configuration, regardless of the values given to the set of free parameters (provided that F^{rep} and F^{attr} satisfy the condition given in Eq. (29)). In particular, the characteristic stable dimensions of the particle system are, in all cases $d_\infty = 0.3$ m and $D_\infty = 3.75$ m. These values, as well as the range of time needed for the patterning, are the same obtained in

the previous section, i.e., with the assumption of an Euclidean metric-based alignment mechanism. In this respect, we can speculate that the asymptotic spatial organization of the particle system is completely determined by the repulsive part of the pairwise interaction kernel (and by the relative coefficient R^{rep}, see also comments in [4]). The hypothesis underlying the flight synchronization process, as well as the resulting variation of the attractive velocity component, does not instead have an effect on the patterns of the large-time insect distribution. By comparing Figs. 7 and 11, it is also possible to notice that in the first case, as commented in the previous section, the specific set of parameter values have an effect on the temporal dynamics of stabilization, whereas in the second case, i.e., in the case of a topological neighborhood metric-based alignment mechanism, the evolution of $d_{\min}$ coincides for all the combination of coefficients taken into account.

Fig. 12 shows the system migratory determinants in the case of the parameter setting $T1$: in particular, for representative purposes, we plot the evolution of X_{swarm} and V_{swarm} resulting from $a = 4$ (i.e., no swarming nor directional flight) and $a = 5$ (i.e., swarming and directional flight). We can observe that, also in the case of this second assumption on bee alignment, the productive motion (indicated by a drop of X_{smarm}) substantially starts after the stabilization of the bee configuration. Exactly the same dynamics have been replicated in the cases of the other coefficient combinations Tk, with $k = 2, ..., 5$.

In contrast to the assumption investigated in Section 3.1, we can however observe that, a topological neighborhood metric-based synchronization hypothesis results in the fact that the migratory behavior of the swarm depends on the value of all the free model parameters (and not only to the one relative to the alignment velocity itself). As shown in Fig. 13, the threshold value of a, say $\bar{a}$, needed to have swarming and productive motion in fact depends on the ratio $F^{\text{rep}}/F^{\text{attr}}$. In particular, increments in the ratio $F^{\text{rep}}/F^{\text{attr}}$ result in increments in $\bar{a}$.

Further, it is interesting to notice that, regardless of the value of $F^{\text{rep}}/F^{\text{attr}}$, the phase transition (i.e., swarming vs. no swarming) of the insect collective migratory behavior is obtained by substantially low values of the communication rate a (i.e., $\bar{a} \leq 13$), i.e., significantly lower than the total amount of component individuals, see again Fig. 13. In this respect, we are observing a *diffusion of information* within the swarm: the knowledge of the direction towards the target destination in fact first passes from the leader to its closest a-th individuals and then gradually to the rest of the population. This is

in contrast with respect to what happens in the previous set of simulations, where a productive collective motion required that $R^{\text{align}} \geq D_{\infty}$, i.e., that all bees simultaneously align to almost the rest of the groupmate (included the leader).

The different swarm phenomenologies resulting from the two alignment hypothesis reflect also on the characteristic time of the insect migratory dynamics. As shown in the representative plot in Fig. 14, the complete alignment of the bee population (i.e., $V_{\text{swarm}} = 0$) is significantly delayed in the case of a topological neighbourhood metric-based synchronization hypothesis. This observation is a further confirmation that, in the hypothesis investigated in this section, the information of the direction of movement gradually diffuses within the population, whereas in the other case, there is simultaneous flight synchronization, which involves almost all individuals at the same time.

4. Inclusion of random contributions

The numerical results proposed so far have been obtained by neglecting the random terms in Eq. (5): we have indeed constantly assumed that all bees completely apply the given rules of motion. However, unconscious fluctuations may characterize individual behavior.

In this respect, for each insect i we add a fluctuation velocity term, given by a vector ξ_i, whose modulus and direction are, at any time t, random variables which uniformly fall within the ranges of values $[0, v_{\text{rand}}]$ (with $v_{\text{rand}} \leq v_{\text{max}}$) and $[0, 360^{\circ})$, respectively. As it is possible to see by comparing the plots in Fig. 15, which describe the swarm patterning and migratory determinants in the representative cases $M6$ (left panels) and $T1$ with $a = 5$ (right panels), the inclusion of random fluctuations in bee dynamics does not have an effect on the swarm organization in a stable crystalline pattern. However, when the maximal possible modulus of the random velocity component is large enough, i.e., $v_{\text{rand}} = v_{\text{max}}$, the insect cloud undergoes uncorrelated (and therefore not productive) movement. In contrast, if $v_{\text{rand}} \ll v_{\text{max}}$, the collective dynamics of the swarm are still characterized by fluctuations, which however do not have a dramatic effect on the asymptotic behavior of the system, in term of collective synchronized flight.

The obvious rationale underlying such a phenomenology is that, when $v_{\text{rand}} = v_{\text{max}}$, the fluctuation term ξ_i overcomes the other velocity contributions in Eq. (5), thereby preventing the normal behavior of the swarm.

However, too large values of v_{rand} are not reasonable, since they only have to implement unconscious individual deviations from the exact application of the set rules of flight.

5. Conclusion

The collective and coordinated motion of groups of animals has been recently become of increasing interest for the modeling community. In the last decades, this field has been treated with different approaches, that can be classically classified in continuous, discrete, and kinetics models, as specified in the Introduction. In this perspective, a microscopic-discrete mathematical model has been here proposed to describe selected dynamics of a bee swarm. Each insect has been assumed to behave according to the so-called first principles of motion, which involve social interactions, such as the tendency to remain within the population while keeping a comfort distance from the other individuals, and the ability to synchronize the flight with the surrounding groupmates. These ideas have been translated in a first-order mathematical model based on a set of ODEs, each of them describing the evolution of the position of a bee. In particular, long- and short-range particle pairwise interactions introduce non-locality in the individual behavior.

The resulting model has been used to test some assumptions underlying insect social behavior. In particular, we have focused either on an Euclidean metric-based or on a topological neighborhood metric-based alignment mechanism, which impact also on the definition of the attraction/repulsion velocity components. In more details, we have analyzed, in each of the two cases, the model behavior in different regions of the parameter space. In this respect, given the intrinsic multiparametric nature of the model components, we have taken advantage of some theoretical studies on the H-stability of particle interaction kernels, discussed in [4], [22], and here extended to the proposed velocity functions, following the calculations proposed in [6] in the case of cell systems. The concept of H-stability was introduced in statistical mechanics [39] and it is closely related to the asymptotic configuration of discrete systems. More specifically, from the above-cited works, we can recall the following theoretical results: given a population of n agents, whose dynamics are determined by a pairwise interaction potential, say u, we have that: (i) if u is not H-stable (or *catastrophic*), then the minimal interparticle distance at the equilibrium collapses to 0 when the total amount of individuals n goes to infinity; (ii) if u is H-stable, then the minimal interparticle

distance at the equilibrium is bounded by finite strictly positive values, regardless the number of individuals n. In this last case, if n goes to infinity, the system distribution explodes. Since the present article has been focused on swarming phenomenology, which are characterized by a finite number of agents with a well-defined spacing maintained within the bee cloud during flight, it has been necessary to avoid catastrophic situations, i.e., to assure the H-stability of the attractive/repulsive kernels employed to describe insect behavior. As previously explained, such an analytical approach, in conjunction with empirical observations, has been able also to restrict the range of value variations of the free model parameters, which have to assure a realistic crystalline configuration of the swarm.

Given the definition of some migratory determinants to classify the resulting collective phenomenology of the bee population, our results have first shown that, in the case of the Euclidean metric-based alignment process, the asymptotic distribution of bees within the cloud is independent from the specific set of parameter values (provided the condition for the H-stability of the interaction kernels). On the opposite, the collective migratory determinants dramatically and entirely rely on the extension of the synchronization region, which has to be in the range of the asymptotic dimensions of the bee cloud to have swarming and collective behavior.

We have then turn to analyze swarm phenomenology in the case of a topological neighborhood metric-based alignment mechanism, which impacts on the definition of the adhesive velocity component. In this respect, we have observed that the asymptotic configuration of the swarm remains unaltered with respect to the previous modeling assumption. This is indicative of the fact that the characteristic dimensions of the stable pattern are entirely determined by the repulsive part of the interaction kernel. The set of simulations proposed in Section 3.2 have also shown that the migratory dynamics of the bee population depend both on the ratio $F^{\text{rep}}/F^{\text{attr}}$ and on the communication rate a, i.e., on the values of the three free model parameters. However, in all the analyzed cases, the threshold number of individuals that each bee has to consider to have a productive swarming is substantially small (i.e., $\bar{a} \leq 13$), in contrast to the case of an Euclidean metric-based synchronization mechanism, where the alignment region had to include almost the entire cloud to observe an effective directional flight. A topological neighborhood metric-based migratory assumption indeed results in a gradual diffusion of information within the bee population: this has been also confirmed by the greater time needed by the swarm to completely align with respect to the

case of the Euclidean metric-based synchronization hypothesis. We have also discussed the role of possible random fluctuations in bee velocity.

It is finally interesting to notice that in our study we have not observed hybrid swarm phenomenologies (e.g., swarming without productive motion or *vice versa*), which are in principle possible and have been captured by other similar models [9].

We here remark that, in principle, the computational results presented in the previous part of the paper depend on the initial condition of the particle system. However, we have observed that the simulation outcomes obtained by keeping the same initial density of bees (i.e., the initial diameter of the swarm and number of insects), while randomly varying the initial individual position, did not significantly differ. For instance, the values of the standard deviations relative to swarm migratory determinants (e.g., asymptotic velocity and barycenter displacement) fell in the range [2 , 4] %, if evaluated over at least 10 different and independent simulations. In this respect, each plot in Section 3 has reproduced the results of a single representative numerical realization. The absence of error bars in the figures, according to us, also avoids unnecessary graphical overcomplications of the presented figures.

Comparison with pertinent literature. As explained in the Introduction, our model belongs to the class of microscopic/discrete approaches dealing with collective dynamics of animal populations. Of this group of methods, some are devoted to reproduce selected features of bee swarming. It is indeed important to discuss their differences and similarities with respect to our approach.

We first remark that most of the discrete models presented in the literature are based on the already-introduced set of first principle of swarming [9], i.e., attraction/cohesion, avoidance, and alignment.

Entering in more details, in [28], Fetecau and Guo implement a second-order model, where attraction and repulsion stimuli are described by a Morse potential, whereas the alignment process of a given bee involves its two-fold faster neighbors (with an effect that decreases with the mutual distance between the pair of interacting insects, according to a quite complex, tanh-based, rule). Bee dynamics also account for a random component, which is active only when the interaction of an individual with the rest of the swam is low enough. The authors introduce a visual field for each bee, given by a planar cone which is constantly aligned to the direction of motion and formed by two regions: a central cone where the other individuals are set to be seen

directly, and therefore assigned a unit weight, and a peripheral area where the other individuals are set to be seen partially, and therefore assigned a lower weight. In our model, a peripheral vision is not considered, since it is known from biology that the compound eyes of bees cover most of the front and of the sides of their head, assuring an almost homogeneous vision. Fetecau and Guo finally differentiate a subpopulation of leader bees, that do not interact with their groupmates and are assigned an oscillatory motion. They in fact first fly towards the nest; then, once reached the leading edge of the swarm, they turn back to the trailing part of the population (at a lower velocity and visibility).

Attraction, repulsion, and alignment are also at the basis of the first order model presented in [36]. Entering in more details, the cohesion velocity contribution is modeled as a vector pointing from the position of each bee to the center of mass of the set of neighboring insects which fall within its visual distance. In this respect, we have here preferred to implement pairwise interaction kernels, since it is difficult to establish whether a bee exactly knows the position of the barycenter of the rest of groupmates. The alignment rule instead relies on an Euclidean metric-based assumption, namely each bee is set to synchronize its movement with all the seen groupmates (regardless of their speed). This is quite similar to the assumption tested in Section 3.1, even if in our case the region of attraction and alignment do not coincide. As in the case of the work by Fetecau and Guo, also in [36], a set of leader bees is defined and assigned a back-and-forward motion within the swarm, in order to diffuse the information of the productive direction to the overall population.

In [26], the authors describe both the decision-making process used by the house-hunting honeybees to find a new nest site and their guidance role within the rest of the swarm. Focusing on the latter, we can notice that Diwold and colleagues employ a cohesion term that makes each bee attracted by the barycenter of a set of fast enough individuals, which are also involved in a topological metric-based alignment mechanism. Such an assumption on flight synchronization is similar to our second hypothesis (tested in Section 3.2) although we have here implemented different interaction velocity components. The resulting model is then applied to compare the swarming of two different species of honeybees, namely *Apis Mellifera* and *Apis Florea*. In particular, while *A. Mellifera* is a cavity-nesting species, whereas *A. Florea* is an open-nesting species. This means that the *Apis Mellifera* has to find a roomy and comfortable homesite, protected from cold winds and from

predators. Conversely, *A. Florea* usually nests on a shaded branch, having less constraints in finding a suitable location.

A more general (i.e., not strictly related to bee dynamics) model is proposed in [17]. It focuses on two aspects: how information is transferred among moving groups of animals and how they can find an agreement when informed individuals suggest different moving directions to rest of the population. Such an approach still relies on the classical social principle of attraction/repulsion and alignment. In particular, the unexpected conclusion is that the larger is the animal group the smaller is the necessary proportion of informed individuals required to have a productive collective movement. This is a very interesting result, whose applicability to the case of bee swarms should be investigated. The same research group proposes also a model that focuses on the pattern characteristic of animal populations [18]. Their approach includes a Morse potential that, in a given range of parameters, satisfies the H-stability conditions (thereby assuring a crystalline configuration) and two additional terms: they are relative to self-propulsion and friction and their balance results in the capability of the system to reach an asymptotic collective speed (as it happens also in our model in given regimes of free parameters).

Finally, in [20], [21], Cucker and Smale present a well-known model able to realistically capture flocking phenomenology: more specifically, their approach includes the emergence of temporary leader individuals and is based on a term relative to movement synchronization mechanisms, which are affected by a communication rate depending on the interindividual mutual distances.

The dichotomy between topological metric- vs. Euclidean metric-based interactions between animals belonging to the same population is the topic of a very interesting article by Ballerini and coworkers, who deal with flocking events of European Starling swarms under external perturbations (e.g., predator attacks) [1]. More specifically, these authors experimentally demonstrate, by an analysis of a large amount of photographic data, that each individual interacts with a fixed number of groupmates (6-7) and not with all neighbors falling within a given region. In other words, the collective and coordinated migration of bird colonies is the result of topological interactions, as also confirmed by the computational results proposed in the same work, which are obtained with an agent-based model.

The observations by Ballerini and colleagues well fit with the focus of our work. In particular, it would be interesting to perform their empirical

study in the case of bee colonies, in order to point out if topological arguments are involved in bee swarming as well. In this respect, it would be relevant (but very difficult) to address two further points: (i) if topological-based interactions underly only attractive/repulsive insect behavior or also flight synchronization mechanisms and (ii) if external conditions and/or the objective of migration affect the type of interindividual interactions (e.g., a predator attack may stimulate topological metric-based interactions, whereas exploring or feeding tasks may require Euclidean metric-based interactions).

We can therefore conclude that the main components of our model are already presented in published similar approaches: however, with respect to the literature, we have here tested and compared, in terms of simulation outcomes, alternative assumptions underlying the flight alignment mechanism (which impact also on the definition of the pairwise attractive/repulsive velocity terms) and used analytical arguments to obtain plausible parameter settings, i.e., resulting in realistic crystalline swarm configurations.

Future developments. The proposed model has investigated different social mechanisms underlying the behavior of a bee swarm. However, our approach can be further improved in several directions. We first recall that in our model a given bee is set as a leader for the entire period of observation. This assumption is consistently based on the fact that, as known from the experimental literature, in a bee population there is an immutable hierarchy within the component individuals, i.e., each of them has a specific role. For instance, a small set of informed/streaker insects have already visited the target site and therefore is able to guide the rest of the swarm to the destination. On the opposite, in other animal groups, there is the continuous emergence of temporary leaders, which change in few seconds. A more detailed description of the movement of informed bees, as well as on the diffusion of information to the rest of the swarm, is however needed. In this respect, various assumptions have been proposed to account for the flight guidance mechanism of the leader-follower system. According to the chemical hypothesis, the leaders can pilot the cloud of bees to the target destination by the production of the Nasonov pheromone, which attracts the uninformed insects. Another possible explanation is that the scout bees lead the follower individuals via visual signals. Specifically, Lindauer in 1955 proposed that the leaders can transmit the direction of movement by flying through the swarm [42]. In particular, such informed bees first fly at high speed from the back of the swarm to its front (at an upper layer, where they are more visible in contrast with

the light of the sky). Then, once they have reached the front of the cloud, they slowly come back to the rear edge, along the bottom or the sides of the population to be almost invisible to the groupmates. The entire dynamics finally start again. The non-informed bees in turn align to the leader individuals: the information progressively diffuses in a ripple effect and therefore the swarm heads towards the new location gradually increasing its overall speed. Such a mechanisms has been confirmed by empirical experiments as well [42]. The above-explained assumptions of leader behavior can be easily tested with our approach, also in conjunction with the different hypothesis underlying the alignment process. In this respect, it would also useful to extend the model in three dimensions.

Another aspect that would require more detailed investigation is the possible modification of the social interaction rules due to external conditions (e.g., presence of predators or weather changes). Also the presence of obstacles, such as trees or building structures, may impact on bee behavior. It should be also interesting to study if the phenomenology of the swarm differs according to specific group tasks (e.g., feeding, exploring).

A further model improvement can be represented by the inclusion of bee gazing direction as a further degree of freedom. In this respect, as done in the case of pedestrians [15], for each insect i, it should be defined a unit vector, say $\mathbf{g}_i(t) = (\cos\gamma_i(t), \sin\gamma_i(t))$ (being γ_i the angle between $\mathbf{g}_i$ itself and the x-axis of the domain), defining the direction of its gaze, cf. Fig. 16. $\mathbf{g}_i$ may have also its own evolution equation, accounting for instance head rotation with respect to the direction of motion or towards environmental stimuli (e.g., sounds or light signals) and/or due to unconscious fluctuations. The inclusion of a gaze vector for each insect i would also allow to improve the definition of the visual region Ω_i^{vis} by introducing a proper half visual angle, say θ, which would actually extend from $\mathbf{g}_i$ (see again Fig. 16). In this respect, each individual should be assumed to not consider and therefore interact with the insects out of Ω_i^{vis}. Anisotropy would be indeed introduced in bee dynamics, which would destroy the symmetry of the repulsive/attractive kernels introduced in Eqs. (7)-(8). This would impede the application of the H-stability criterium introduced in [4] and here applied in Theorems 3.1 and 3.2, since it requires that the interaction potentials of interest are isotropic (cf. Hypothesis 3 in [4]). The inclusion of bee gazing direction would therefore require a deeper analytical study. However, we here remark that the bee visual angle is substantially large (i.e., $\approx 320°$, as reported in the experimental literature [43]). It indeed covers almost all directions and therefore each

bee is aware of the presence of almost the entire set of groupmates. In this respect, the hypothesis of a round visual area employed in this work is not too restrictive.

Finally, our approach can be extended to a large swarm, formed by thousands of individuals disposed in almost spheroidal patters. In this respect, it would be interesting to test if the results obtained by varying the alignment mechanisms (and the relative parameters) would apply also in the case of significantly increased numbers of bees. It is useful to remark, however, that the proportion between informed/non-informed individuals set in this model (i.e., 1/99) is in the range of values empirically measured for large swarms (300 to 400 leaders in a swarm of 10000 insects [42]). Obviously, a model extension involving a huge number of particles would cause computational issues, i.e., mainly related to the optimization of computing time. In this respect, a possible solution is represented by the use of serial and parallel computing. High performance serial computing can be achieved by using the same programming techniques employed in particle fluid-dynamic simulations. Otherwise, parallel computing is possible, for example, using Message Passing paradigm (MPI) or shared memory parallelization. In the first case, the computational domain would be divided in subdomains that in turn would be assigned to a single processor. At each time step, each processor should communicate the bees who leave its portion of domain and enter the sub-domain of a neighboring node. In case of a shared memory parallelization (e.g., on GPU devices), the computational domain and the data structure storing population data would be shared among different threads, each of them updating the state of a sub-set of individuals.

Acknowledgements. AC acknowledges partial funding by the Politecnico di Torino and the Fondazione Cassa di Risparmio di Torino in the context of the funding campaign "La Ricerca dei Talenti" (HR Excellence in Research). The Authors also thank Prof. L. Preziosi of the Department of Mathematical Sciences for support and fruitful discussions. AC and MS finally thank Prof. J. A. Carrillo of the Department of Mathematics at the Imperial College of London, with whom they had the original discussion and idea of the possible application of the H-stability criterium in the case of pairwise interaction kernels regulating the behavior of systems of biological individuals.

[1] M. Ballerini, N. Cabibbo, R. Candelier, A. Cavagna, E. Cisbani, I. Giardina, V. Lecomte, A. Orlandi, G. Parisi, A. Procaccini, M. Viale, V.

Zdravkovic, Interaction ruling animal collective behavior depends on topological rather than metric distance: evidence from a field study, Proc. Natl. Acad. Sci. U. S. A., 105(4), 1232 – 1237, 2008.

[2] N. Boeddeker, L. Dittmar, W. Stürzl, M. Egelhaaf, The fine structure of honeybee head and body yaw movements in a homing task, Proceedings of the Royal Society of London B: Biological Sciences, 277(1689), 1899–1906, 2010.

[3] M. Burger, V. Capasso, D. Morale, On an aggregation model with long and short range interactions, Nonlinear Analysis: Real World Applications, 8(3), 939–958, 2007.

[4] J. A. Cañizo, J. A. Carrillo, F. Patacchini, Existence of compactly supported global minimisers for the interaction energy, Arch. Rational Mech. Anal., 217, 1197–1217, 2015.

[5] J. A. Cañizo, J. A. Carrillo, J. Rosado, A well-posedness theory in measures for some kinetic models of collective motion, Math. Models Methods Appl. Sci., 21(3), 515 – 539, 2011.

[6] J. A. Carrillo, A. Colombi, M. Scianna, Adhesion and volume constraints via nonlocal interactions, lead to cell sorting, Submitted (preprint in arXiv), 2017.

[7] J. A. Carrillo, M. R. D'Orsogna, V. Panferov, Double milling in self-propelled swarms from kinetic theory, Kinetic and Related Models, 2, 363–378, 2009.

[8] J. A. Carrillo, M. Fornasier, J. Rosado, G.Toscani, Asymptotic Flocking Dynamics for the kinetic Cucker-Smale model, Preprint UAB.

[9] J. A. Carrillo, M. Fornasier, G. Toscani, F. Vecil, Particle, kinetic, and hydrodynamic models of swarming, Mathematical modeling of collective behavior in socio-economic and life sciences, Birkhäuser Boston, 297 – 336, 2010.

[10] Y. Choi, R. Lui, Y. Yamada, Existence of global solutions for the Shigesada-Kawasaki-Teramoto model with weak cross-diffusion, Discrete and Continuous Dynamical Systems 9(5), 1193–1200, 2003.

[11] Y. L. Chuang, M. R. D'Orsogna, D. Marthaler, A. L. Bertozzi, L. Chayes, State transitions and the continuum limit for a 2D interacting, self-propelled particle system, Physica D, 232, 33–47, 2007.

[12] A. Colombi, M. Scianna, and L. Preziosi. Coherent modelling switch between pointwise and distributed representations of cell aggregates. J. Math. Biol., 74(4), 783 – 808, 2017.

[13] A. Colombi, M. Scianna, and A. Tosin. Differentiated cell behavior: a multiscale approach using measure theory. J. Math. Biol., 71(5), 1049 – 1079, 2015.

[14] A. Colombi, M. Scianna, A. Alaia, A discrete mathematical model for the dynamics of a crowd of gazing pedestrians with and without an evolving environmental awareness, Comp. Appl. Math., 36(2), 1113–1141, 2017.

[15] A. Colombi, M. Scianna. Modelling human perception processes in pedestrian dynamics: a hybrid approach. R. Soc. Open Sci., 4, 160561 (2017).

[16] E. Conway, J. Smoller, Diffusion and the predator-prey interaction, SIAM Journal on Applied Mathematics, 33(4), 673–686, 1977.

[17] I. D. Couzin, J. Krause, N. R. Franks, S.A. Levin, Effective leadership and decision-making in animal groups on the move, Nature, 433(7025), 513–516, 2005.

[18] I. D. Couzin, J. Krause, R. James, G. Ruxton, N. Franks, Collective memory and spatial sorting in animal groups. J. Theor. Biol., 218, 1-11, 2002.

[19] E. Cristiani, B. Piccoli, A. Tosin, Multiscale Modeling of Pedestrian Dynamics, MS and A: Modeling, Simulation and Applications, vol. 12, Springer International Publishing (2014).

[20] F. Cucker, S. Smale, On the mathematics of emergence, Jpn. J. Math., 2, 197-227, 2007.

[21] F. Cucker, S. Smale, Emergent behavior in flocks, IEEE Trans. Automat. Control, 52, 852-862, 2007.

[22] M. R. D'Orsogna, Y. L. Chuang, A. L. Bertozzi, and L. S. Chayes, Self-Propelled Particles with Soft-Core Interactions: Patterns, Stability, and Collapse, Phys. Rev. Lett., 96, 104302, 2006.

[23] P. Degond, S. Génieys, A. Jüngel, A steady-state system in non-equilibrium thermodynamics including thermal and electrical effects, Mathematical methods in the applied sciences, 21(15), 1399–1413, 1998.

[24] P. Degond, S. Motsch, Continuum limit of self-driven particles with orientation interaction, Math. Models Methods Appl. Sci., 18, 1193–1215, 2008.

[25] P. Degond, S. Motsch, Large-scale dynamics of the Persistent Turing Walker model of fish behavior, J. Stat. Phys. 131, 989–1021, 2008.

[26] K. Diwold, T. M. Schaerf, M. R. Myerscough, M. Middendorf, M. Beekman, Deciding on the wing: in-flight decision making and search space sampling in the red dwarf honeybee Apis florea, Swarm Intelligence, 5(2), 121–141, 2011.

[27] D. Drasdo, On selected individual-based approaches to the dynamics of multicellular systems, In Multiscale Modeling, Eds. W. Alt and M. Griebel, Birkhäuser, 169–203 (2005).

[28] R. C. Fetecau, A. Guo, A mathematical model for flight guidance in honeybees swarms, Bulletin of mathematical biology, 74(11), 2600–2621, 2012.

[29] H. Von Foerster, Some remarks on changing populations, The kinetics of cellular proliferation, 382–407, 1959.

[30] M. Fornasier, J. Haskovec, G. Toscani, Fluid dynamic description of flocking via Povzner-Boltzmann equation, Physica D: Nonlinear Phenomena, 240(1), 21–31, 2011.

[31] G. Galiano, A. Jüngel, J. Velasco, A parabolic cross-diffusion system for granular materials, SIAM Journal on Mathematical Analysis, 35(3), 561–578, 2003.

[32] I. Giardina, Collective behavior in animal groups: theoretical models and empirical studies, HFSP Journal, 2, 205–219, 2008.

[33] W. Gurney, S. Blythe, R. Nisbet, Nicholson's blowflies revisited, Nature, 287:17–21, 1980.

[34] S. Y. Ha, J. G. Liu, A simple proof of the Cucker-Smale flocking dynamics and mean-field limit, Comm. Math. Sci., 7, 297–325, 2009.

[35] S. Y. Ha, E. Tadmor, From particle to kinetic and hydrodynamic descriptions of flocking, Kinetic and Related Models, 1, 415–435, 2008.

[36] S. Janson, M. Middendorf, M. Beekman, Honeybee swarms: how do scouts guide a swarm of uninformed bees?, Animal Behaviour 70(2), 349–358, 2005.

[37] J. Kim, Smooth solutions to a quasi-linear system of diffusion equations for a certain population model, Nonlinear Analysis: Theory, Methods & Applications, 8(10), 1121–1144, 1984.

[38] Y. Kuang, S. Gourley, Wavefronts and global stability in a time-delayed population model with stage structure, Proceedings of the Royal Society of London A: Mathematical, Physical and Engineering Sciences, 459(2034), The Royal Society, 2003.

[39] D. Ruelle. Statistical mechanics: Rigorous results. W. A. Benjamin, Inc., New York-Amsterdam, (1969).

[40] K. M. Schultz, K. M. Passino, T. D. Seeley, The mechanism of flight guidance in honeybee swarms: subtle guides or streaker bees?, Journal of Experimental Biology, 211(20), 3287–3295, 2008.

[41] M. Scianna, L. Preziosi, Multiscale developments of the cellular Potts model, Multiscale Model Simul, 10(2), 342 – 382, 2012.

[42] T. D. Seeley, Honeybee democracy. Princeton University Press (2010).

[43] R. Seidl, W. Kaiser, Visual field size, binocular domain and the ommatidial array of the compound eyes in worker honey bees, Journal of comparative physiology 143(1), 17–26, 1981.

[44] D. J. T. Sumpter, Collective animal behavior. Princeton University Press (2010).

[45] J. Toner, Y. Tu, Long-range order in a two-dimensional dynamical xy model: How birds fly together, Phys. Rev. Lett., 75:4326–4329, 1995.

[46] C. M. Topaz, A. L. Bertozzi, Swarming patterns in a two-dimensional kinematic model for biological groups, SIAM J. Appl. Math., 65, 152 – 174, 2004.

[47] C. M. Topaz, A. L. Bertozzi, M. A. Lewis, A nonlocal continuum model for biological aggregation, Bulletin of Mathematical Biology, 68, 1601 – 1623, 2006.

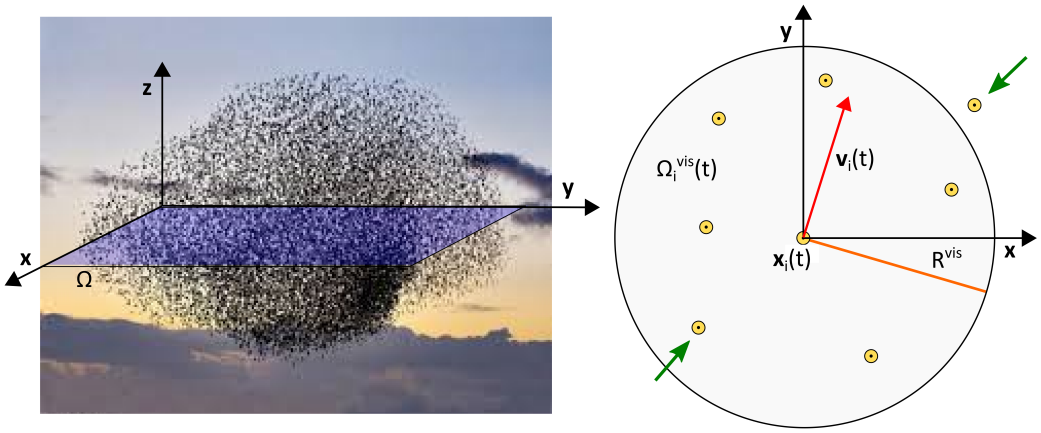

Figure 1: Left panel: The virtual population of bees is modeled in the two-dimensional space $\mathbb{R}^2$, i.e., we are taking into account a planar section of a typical swarm. Right panel: Each bee i is represented as a material point and characterized by its actual position $\mathbf{x}_i(t)$ and velocity $\mathbf{v}_i(t)$. For each insect, we also define a visual region $\Omega_i^{\rm vis}(t)$, i.e., a round area determined by the bee visual depth $R^{\rm vis}$. The inclusion of a visual field implies that each bee is not able to see and therefore to interact with the entire set of their groupmates (see the individual indicated by the green arrow). For representative purposes, hereafter the virtual bees will be indicated by rigid disks centered at their actual position.

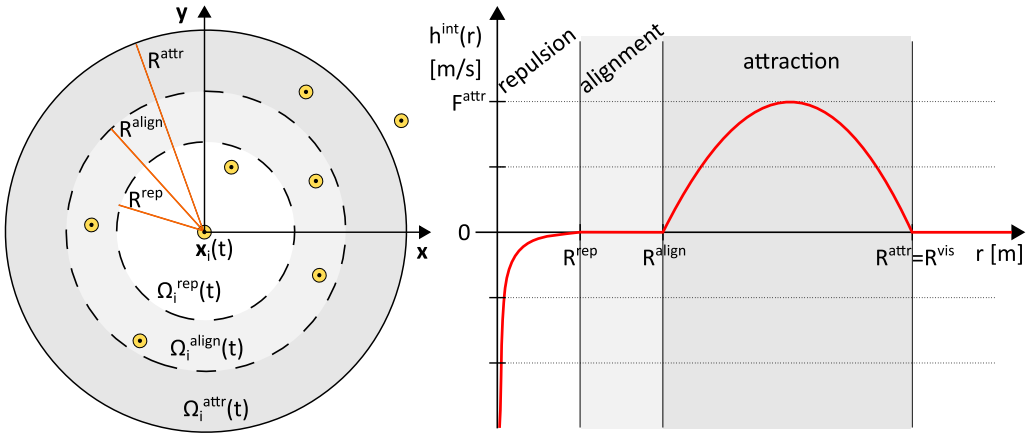

Figure 2: Euclidean metric-based alignment mechanism. Left panel: Representation of the three interaction regions: the repulsive neighborhood $\Omega_i^{\rm rep}(t)$ (see Eq. (12)), the alignment neighborhood $\Omega_i^{\rm align}(t)$ (see Eq. (13)), and the attractive neighborhood $\Omega_i^{\rm attr}(t)$ (see Eq. (14)). In particular, assuming $R^{\rm attr} = R^{\rm vis}$, we have that the three interaction regions entirely cover the visual field of each animal, i.e., $\Omega_i^{\rm rep}(t) \cup \Omega_i^{\rm align}(t) \cup \Omega_i^{\rm attr}(t) = \Omega_i^{\rm vis}(t)$. Right panel: Plot of the pairwise interaction kernel $h^{\rm int} : \mathbb{R}_+ \longmapsto \mathbb{R}$ given by the sum of the repulsive and attractive functions defined in Eqs. (15)-(16), i.e., $h^{\rm int}(r) = h^{\rm rep}(r) + h^{\rm attr}(r)$.

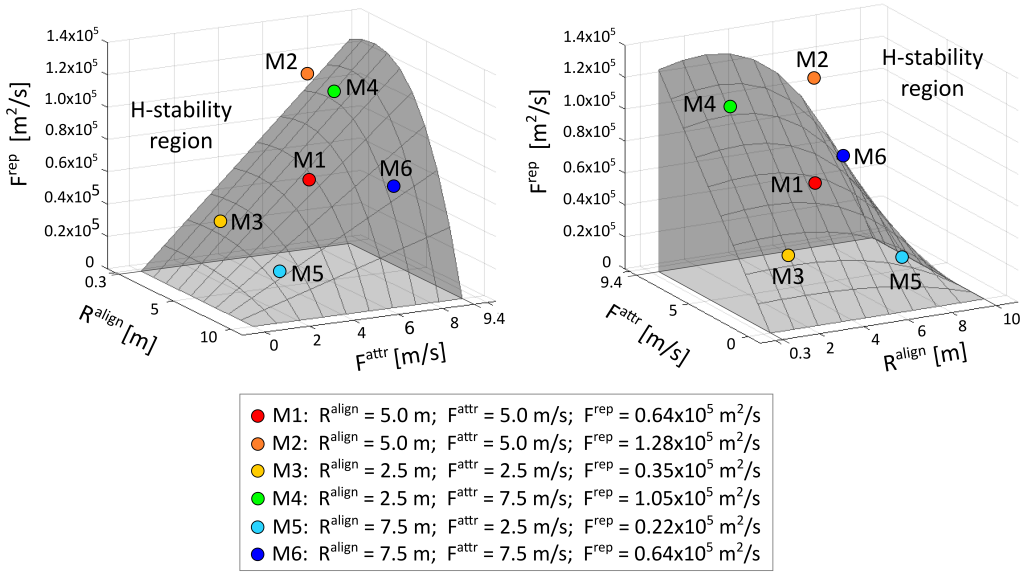

Figure 3: Euclidean metric-based alignment mechanism. Different views of the permitted parameter region, i.e., where h^{int} is H-stable. The space of free model coefficients is given by $(R^{\text{align}}, F^{\text{rep}}, F^{\text{attr}}) \in \mathbb{R}^3_+$. In particular, biological considerations allows the following restrictions: $R^{\text{align}} \in [R^{\text{rep}}, R^{\text{attr}}]$ and $F^{\text{attr}} \in [0, v_{\max}]$. The H-stability criterium in Eq. (17) further reduces the possible variations of parameter values to the region above the grey surface. Of the remaining combination of coefficients, we focus on the six sets Mk, where $k = 1, ..., 6$, since they are sufficiently distributed, thereby covering large enough parameter regimes.

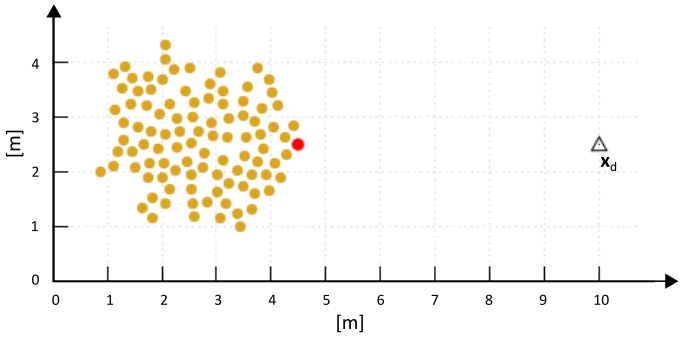

Figure 4: Initial spatial configuration of the swarm. The red disk denotes the position of the informed (leader) bee, while the other individuals are represented by yellow disks. The target destination $\mathbf{x}_d$ =(10 m, 2.5 m) is here represented by a triangle.

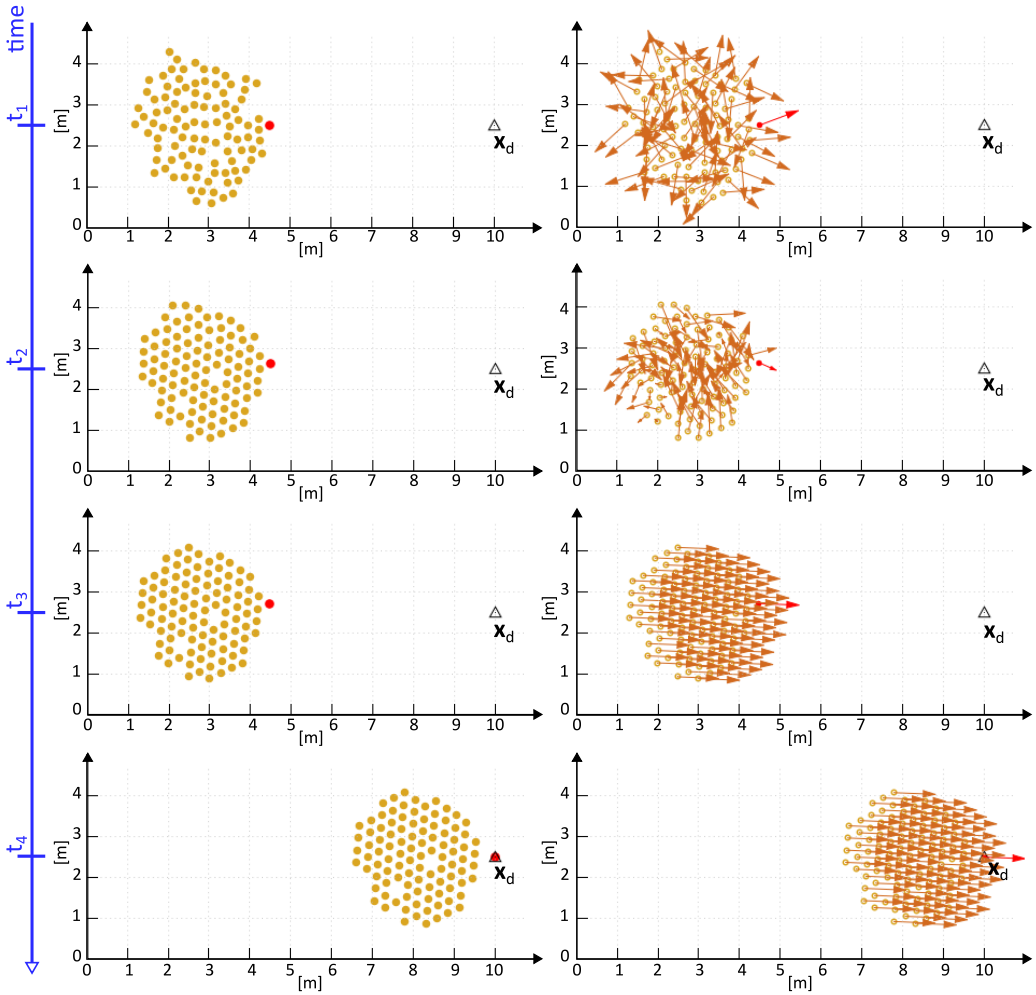

Figure 5: Representative evolution of the bee population in the case of swarming and productive movement. Left panels show the position of the insects at selected different times, right panels show also their direction of motion (i.e., the unit vector of their velocity, indicated by the orange arrow) at the same instants. It is possible to see that the bee cloud first undergoes crystallization (i.e., $t_1 \to t_2$) and then flight alignment and productive movement, i.e., behind the leader individual towards the target destination (i.e., $t_3 \to t_4$). Such a representative system evolution is obtained with the parameter combination $M6$: however, it is completely consistent for all the other analogous cases.

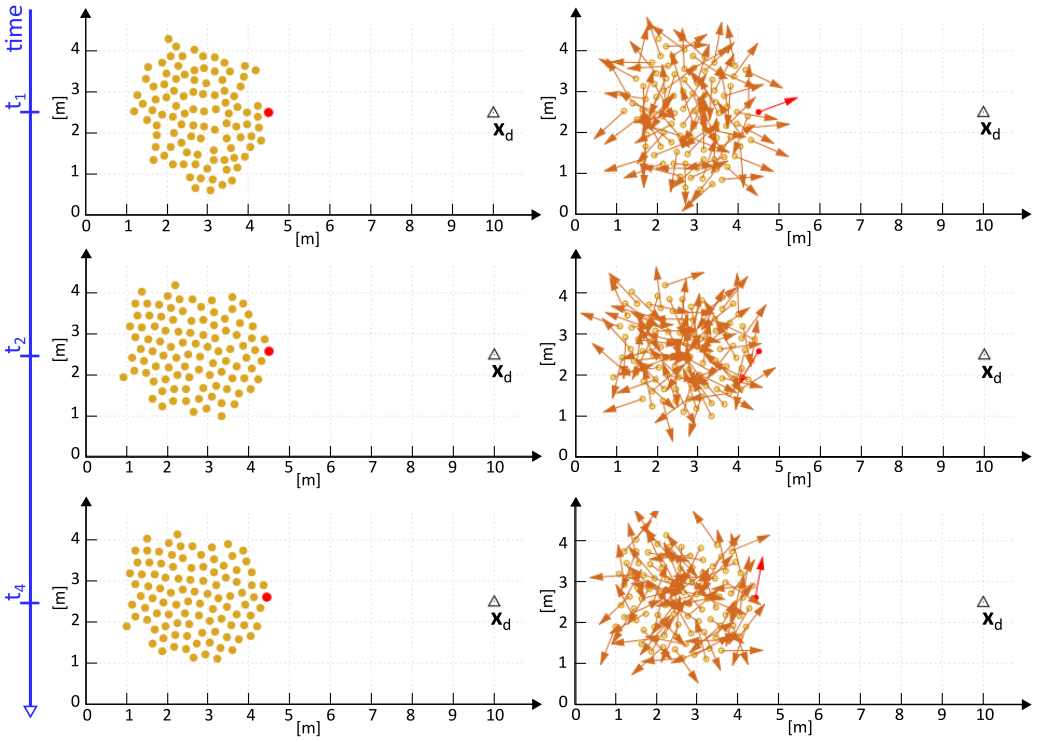

Figure 6: Representative evolution of the bee population in the case of uncorrelated and non productive behavior. Left panels show the position of the insects at selected different times, right panels show also their direction of motion (i.e., the unit vector of their velocity, indicated by the orange arrow) at the same instants. It is possible to see that the bee cloud still organizes in a crystalline pattern (i.e., $t_1 \to t_2$), however the insect velocities do not align: therefore, the bee cloud almost fluctuates around the initial position (compare the position of the insects at the final time t_4 here and in the previous Fig. 5). Such a representative system evolution is obtained with the parameter combination $M4$: however, it is completely consistent for all the other analogous cases.

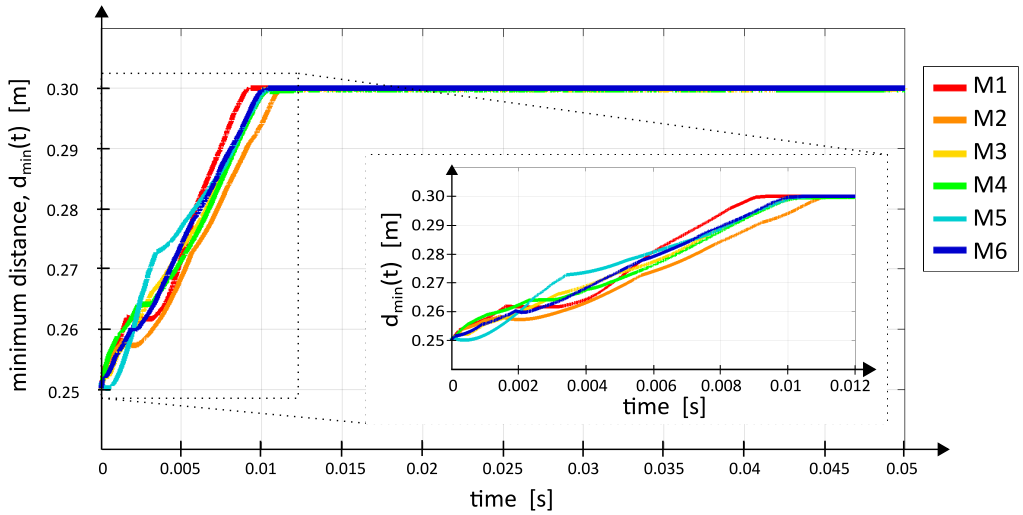

Figure 7: Euclidean metric-based alignment mechanism. Time evolution of the minimal distance between pairs of bees, i.e., $d_{\min}(t)$, observed in selected combinations of parameters. We can first notice that, in all cases, $d_{\min}$ converges to $d_\infty = 0.3$ m, the swarm constantly organizes in a crystalline-like configuration. This is consistent to the fact that all sets of coefficients satisfy the criterium in Eq. (17) for the H-stability of the system. The specific parameter values instead affect the convergence dynamics: for instance, comparing the cases $M1$ and $M2$, it emerges that higher values of F^{rep} increase the time needed by the swarm to stabilize in the crystalline pattern.

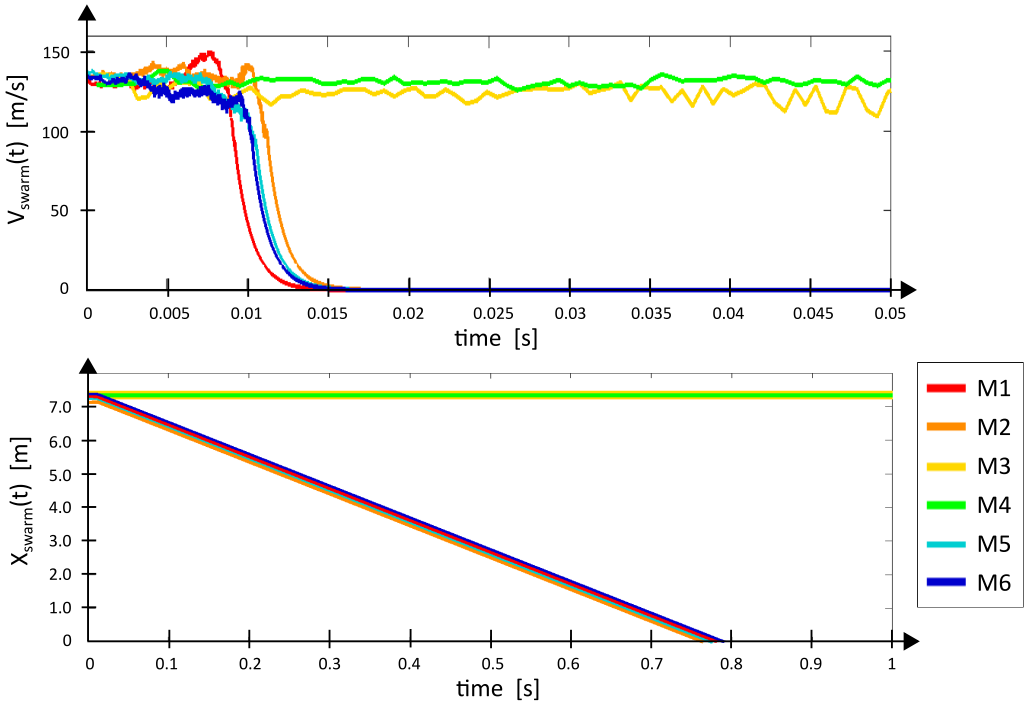

Figure 8: Euclidean metric-based alignment mechanism. Time evolution of V_{swarm} (top panel) and X_{swarm} (bottom panel), introduced in Eqs. (22-23), observed in selected combinations of parameters. It is possible to notice that the bee population undergoes swarming and productive motion only in the cases $M1$, $M2$, $M5$, and $M6$, which are characterized by a sufficiently large R^{align}, i.e., larger than $D_\infty = 3.75$ m.

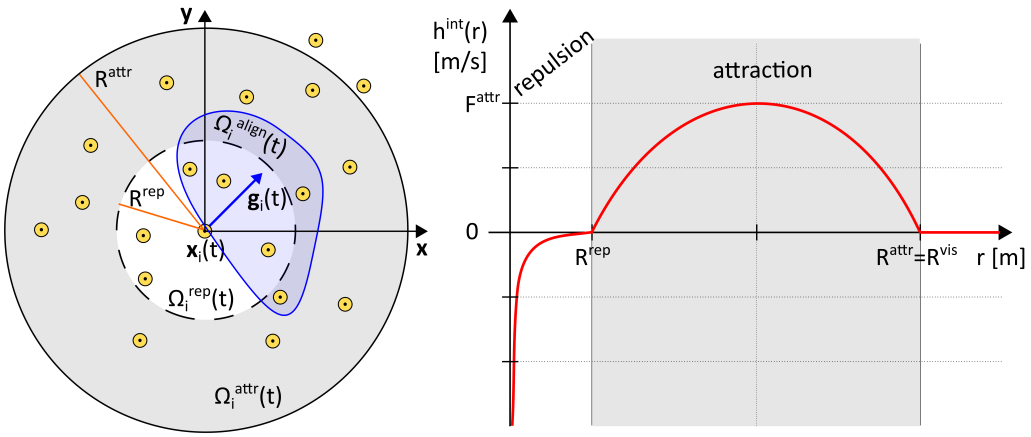

Figure 9: Topological neighborhood metric-based alignment mechanism. Left panel: Representation of the attractive and repulsive regions, defined in Eqs. (25)-(26), and of the alignment set, introduced in Eq. (24). In particular, assuming $R^{\text{attr}} = R^{\text{vis}}$, we have that $\Omega_i^{\text{rep}}(t) \cup \Omega_i^{\text{attr}}(t) = \Omega_i^{\text{vis}}(t)$ for all bees $i = 1, ..., N$ and for any t. Right panel: Plot of the pairwise interaction kernel $h^{\text{int}} : \mathbb{R}_+ \longmapsto \mathbb{R}$ given by the sum of the repulsive and attractive functions defined in Eqs. (27)-(28), i.e., $h^{\text{int}}(r) = h^{\text{rep}}(r) + h^{\text{attr}}(r)$.

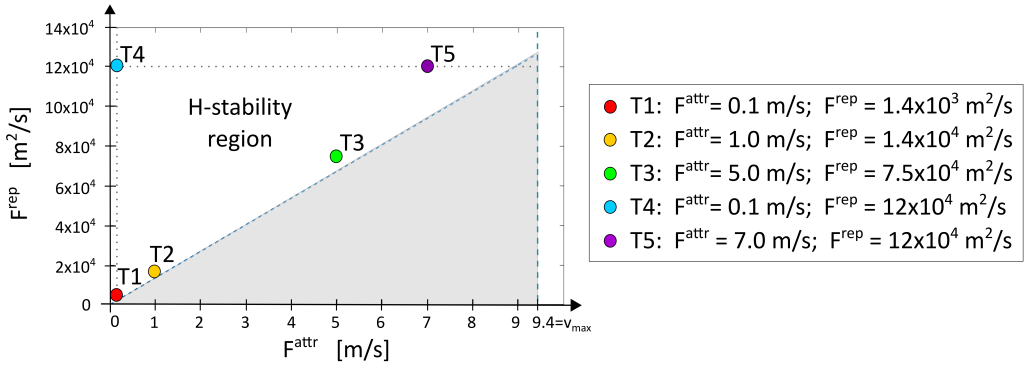

Figure 10: Topological neighborhood metric-based alignment mechanism. The space of free model coefficients is given by $(F^{\text{rep}}, F^{\text{attr}}, a) \in \mathbb{R}^2_+ \times \{1, ..., N-1\}$, being N the total number of insects. In particular, biological considerations allows also the following restriction: $F^{\text{attr}} \in [0, v_{\max}]$. The H-stability-related criterium in Eq. (29) further reduces the possible variations of parameter vales to the white region of the plane $(F^{\text{rep}}, F^{\text{attr}})$. a can instead vary without affecting the system stability. Of the remaining combination of coefficients, we focus on the sets Tk, where $k = 1, ..., 5$, since they are sufficiently distributed, thereby covering large enough parameter regimes.

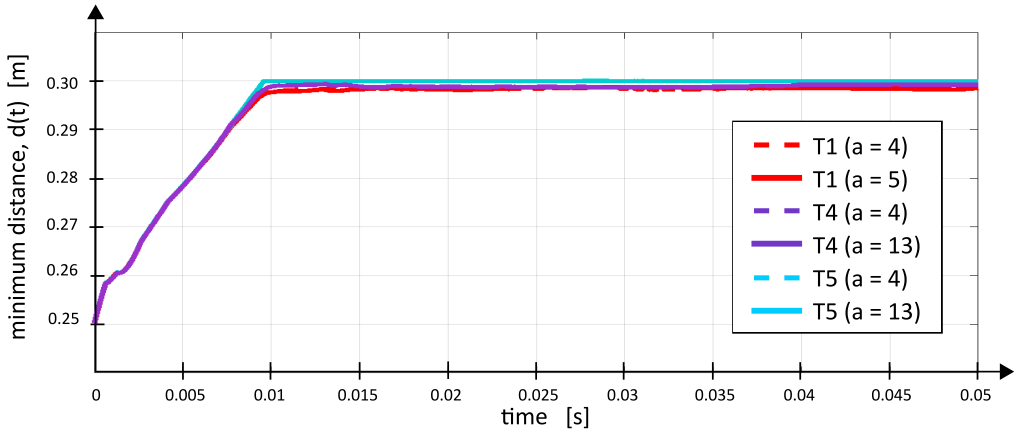

Figure 11: Topological neighborhood metric-based alignment mechanism. Time evolution of the minimal distance between pairs of bees, i.e., $d_{\min}(t)$, observed in selected combinations of parameters. We notice that, in all cases, $d_{\min}$ converges to $d_\infty = 0.3$ m, i.e., the swarm constantly organizes in a crystalline-like configuration. This is consistent to the fact that all sets of coefficients satisfy the criterium in Eq. (17) for the H-stability of the system. Interestingly the asymptotic spatial configuration of the insect is exactly the same obtained in the case of an Euclidean metric-based alignment velocity. This is indicative of the fact that the characteristic dimensions of the large-time pattern are solely determined by the repulsive component of bee dynamics, which is not affected by the variation of the hypothesis underlying the flight synchronization process.

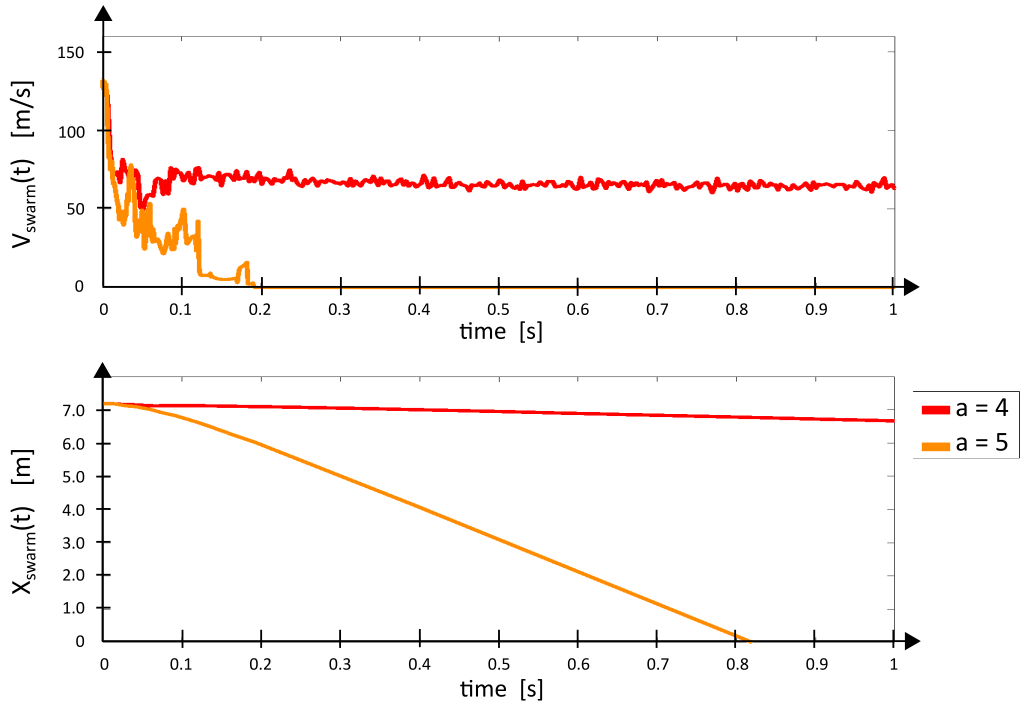

Figure 12: Topological neighborhood metric-based alignment mechanism. Characteristic time evolution of V_{swarm} (top panel) and X_{swarm} (bottom panel) observed in the representative parameter setting $T1$ in the case of swarming and productive motion (i.e., obtained with $a = 4$) or not (i.e., for $a = 5$). Exactly the same dynamics result in the other parameter combinations Tk, with $k = 2, ..., 5$.

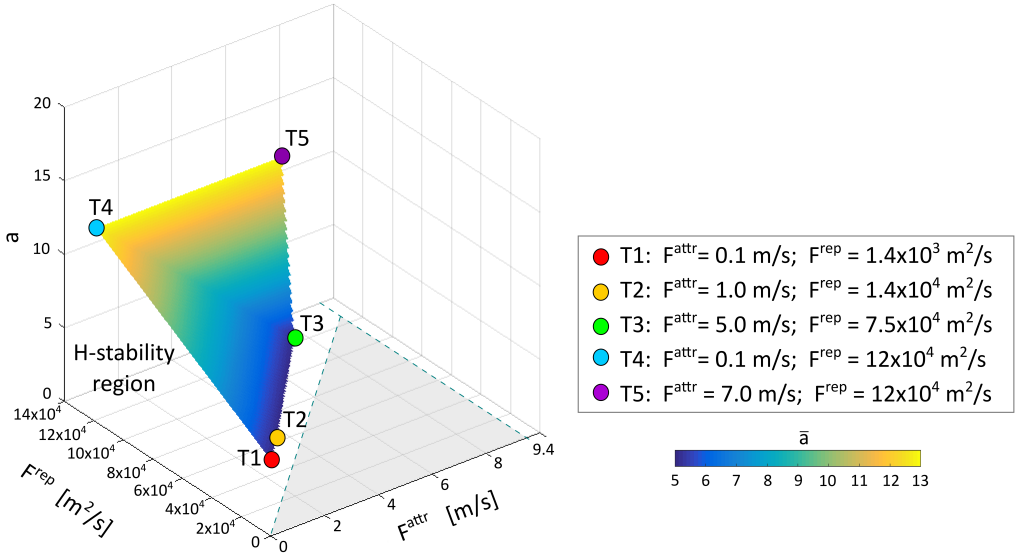

Figure 13: Topological neighborhood metric-based alignment mechanism. For any representative parameter setting Tk (with $k = 1, ..., 5$), the plot shows the threshold value of the communication rate a, i.e., $\bar{a}$, leading to a transition between an uncorrelated individual movement to a swarming behavior with productive motion. It is straightforward to observe that different ratios $F^{\text{rep}}/F^{\text{attr}}$ result in different $\bar{a}$. In particular, increments in the ratio $F^{\text{rep}}/F^{\text{attr}}$ result in increments in $\bar{a}$.

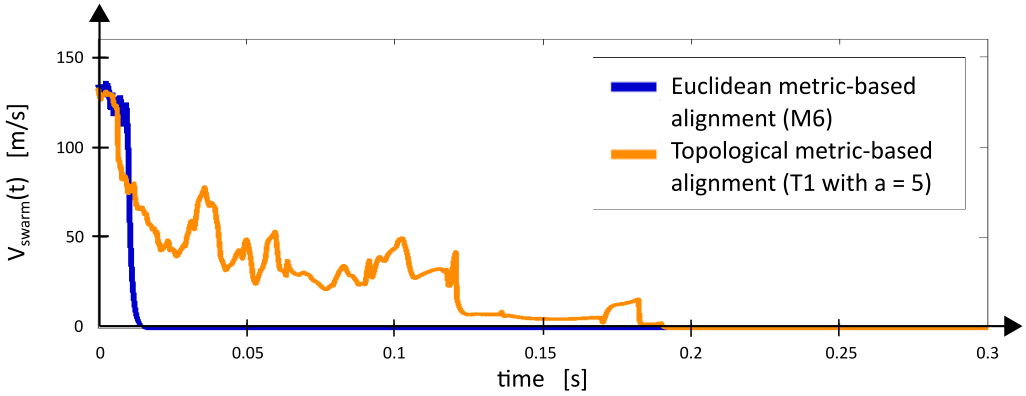

Figure 14: Comparison of the time evolution of V_{swarm} observed in a single representative parameter setting deriving either from the Euclidean or from the topological neighborhood metric-based alignment assumption. The former case is the coefficient combination $M6$, the latter the parameter setting $T1$ with $a = 5$. By comparing the two curves, it is possible to observe that the complete alignment of the bee population is significantly delayed in the case of the topological neighbourhood metric-based synchronization hypothesis, which involves a gradual diffusion of information within the insect cloud rather then a sudden and simultaneous flight alignment.

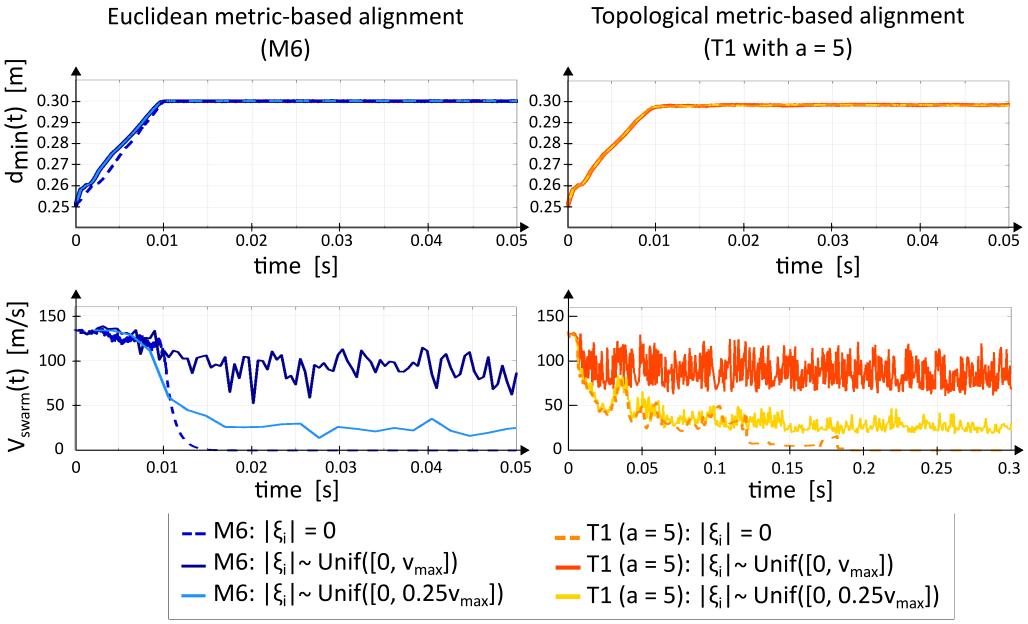

Figure 15: Comparison of the time evolution of $d_{\min}$ (top panels) and of V_{swarm} (bottom panels), observed in representative parameter settings (i.e., $M6$ for the Euclidean metric-based alignment assumption and $T1$ with $a = 5$ for the topological neighborhood metric-based alignment assumption), in the case of addition of the random velocity term ξ_i in Eq. (5), for each bee $i = 1, ..., 100$. As it possible to see, the inclusion of fluctuations does not have an effect on the patterning of the bee swarm, but only on its flight dynamics.

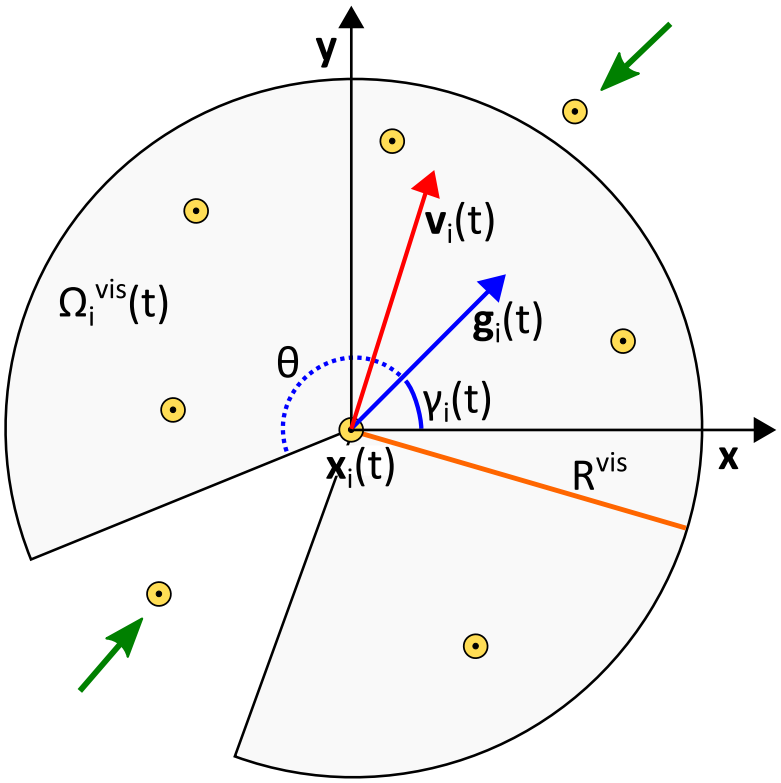

Figure 16: A possible model improvement involves the inclusion of a bee gazing direction, which may be defined by a proper unit vector, say $\mathbf{g}_i$. The inclusion of the insect gaze would also allow to improve the individual visual region, that may be identified by a round sector determined by the visual depth $R^{\rm vis}$ and the half visual angle θ extending from $\mathbf{g}_i$ itself. The definition of such a type of visual field introduces anisotropy in individual behavior.